are involved in the ER-associated ubiquitination system (12). However, the ER stress response has not been intensively studied from the viewpoint of muscular dystrophy. We previously generated and studied mCav3^{P104L} transgenic mice as a model of LGMD1C (13–15). The present study investigates the ER stress response in mCav3^{P104L} transgenic mice as well as a possible gain of function effect of mCav3^{P104L}.

RESULTS

Dose effect of mCav3^{P104L} transgene on the severity of the myopathic phenotype

We previously identified a severe myopathic phenotype in mCav3^{P104L} hemizygous transgenic mice (13). Homozygous mCav3^{P104L} mice were obtained by hemizygous intercrossing and southern blot analysis confirmed the wild-type, hemizygous and homozygous transgenic mouse genotypes (Fig. 1A). Western blot analysis detected less caveolin-3 protein in hemizygous than in homozygous mice (Fig. 1B). We then analyzed the effect of mCav3^{P104L} gene dosages on the myopathic phenotype. Consistent with our previous findings (13), hemizygous mice weighed less than wild-type mice, but the difference did not reach statistical significance. The difference in body weight between homozygous and wild-type mice was statistically confirmed from 4 and 12 weeks of age at all measured points (Fig. 1C). We also found that grip strength significantly differed between the groups from 4 and 12 weeks of age at most measured points (Fig. 1D). Central nucleation or mononuclear infiltration was essentially absent. We measured average areas of myofibers in quadriceps muscles from mice of each genotype (Fig. 1E). Small myofibers were more frequent in the order of homozygous > hemizygous > wild-type mice and non-parametrical statistical analysis confirmed significant differences among the groups (Fig. 1F). The frequency of small myofibers in the gastrocnemius muscle also significantly differed among the genotypes (Supplementary Material, Fig. S1A and B). These data showed that the dose of the mCav3^{P104L} transgene correlated with the severity of the myopathic phenotype.

Residual level of caveolin-3 protein and the myopathic phenotype

The residual amount of caveolin-3 protein in mCav3^{P104L} transgenic mice was <20% of that in wild-type mice (Fig. 1B). To confirm whether other caveolin isoforms counteract the loss of caveolin-3 in muscle cells, we analyzed the expression of caveolin-1 and -2 in mCav3^{P104L} transgenic mice. Messenger RNA levels of caveolin-1 and -2 were increased about 1.5-fold in the skeletal muscle of homozygous mice, whereas no significant change was detectable in hemizygous mice (Fig. 2A and B). Western blotting showed that these changes were consistent at the protein level (Fig. 2C and D). However, immunohistochemistry revealed that upregulated caveolins-1 and -2 were not localized to the sarcolemma, but to the muscle interstitial region containing blood vessels (Fig. 2E). These results indicated that caveolin-1 and -2 upregulation does not compensate for the lack of caveolin-3 function in skeletal muscle. Interestingly, less caveolin-3 protein was detected in hemizygous than in homozygous mice (Fig. 1B). Since the antibodies used for western blotting cannot distinguish between endogenous and mutant caveolin-3 protein, these results suggest that the increased amount of residual mCav3^{P104L} protein in homozygous mice led to more severe myopathy via a toxic gain of function effect.

Localization of mCav3^{P104L} protein and ER stress response

We investigated the subcellular localization of mCav3^{P104L} *in vitro*. Cosmids containing a fluorescent marker for the ER (DsRed-KDEL) or for the Golgi complex (DsRed-Golgi) were cotransfected with wild-type caveolin-3 or mCav3^{P104L} into C2C12 myoblasts. Immunostaining showed surface membrane localization of wild-type caveolin-3, whereas mCAV3^{P104L} did not target the surface membrane and tended to colocalize with the Golgi, but not the ER marker (Fig. 3). The Golgi marker and mCAV3^{P104L} also colocalized in COS7 cells (Supplementary Material, Fig. S2).

We investigated whether mCav3^{P104L} in muscle cells could induce the ER stress response in mCav3^{P104L} transgenic mice by analyzing the expression of genes related to ER stress. Messenger RNA levels of glucose-regulated protein (GRP78), a molecular chaperone in the ER (16), increased 1.5- and 2.5-fold in hemizygous and homozygous mice, respectively, compared with wild-type mice (Fig. 4A and C). Western blotting also confirmed GRP78 induction at the protein level (Fig. 4B and D). Eukaryotic initiation factor 2α (eIF2α) is phosphorylated in response to GRP78 induction under ER stress (17,18). Although the total amount of eIF2α did not significantly change, the amount of phosphorylated eIF2α was increased in transgenic compared with wild-type mice (Fig. 4B and E). We then evaluated the mRNA levels of C/EBP homologous protein (CHOP), which is a pre-apoptotic transcription factor that functions downstream of phosphorylated eIF2α (18,19), and found that they were significantly increased in mCav3^{P104L} transgenic mice (Fig. 4A and C). Overall, these results suggested that mCav3^{P104L} accumulates in the Golgi complex and induces the ER stress response mediated by the molecular chaperone GRP78 and its downstream pathway.

ER stress response toward apoptosis in myofibers from mCav3^{P104L} transgenic mice

We compared the consequences of the mCav3^{P104L}-induced ER stress response using terminal transferase dUTP nick end labeling (TUNEL) assays of quadriceps muscles from mCav3^{P104L} transgenic mice and other mouse models of muscular dystrophy, namely *mdx* and *dy* mice (Fig. 5A). Several TUNEL-positive nuclei of interstitial cells were located outside the myofibers of *mdx* mice and *dy* mice. To distinguish these cells from apoptotic myofibers, we counted the number of myofibers with TUNEL-positive nuclei. Unlike *mdx* mice and *dy* mice, TUNEL-positive nuclei in mCav3^{P104L} transgenic mice were mainly located inside myofibers. Although the average number of TUNEL-positive myofibers was increased in mCav3^{P104L} transgenic mice, the increase was modest compared with the amount in *mdx* mice and *dy* mice (Fig. 5B).

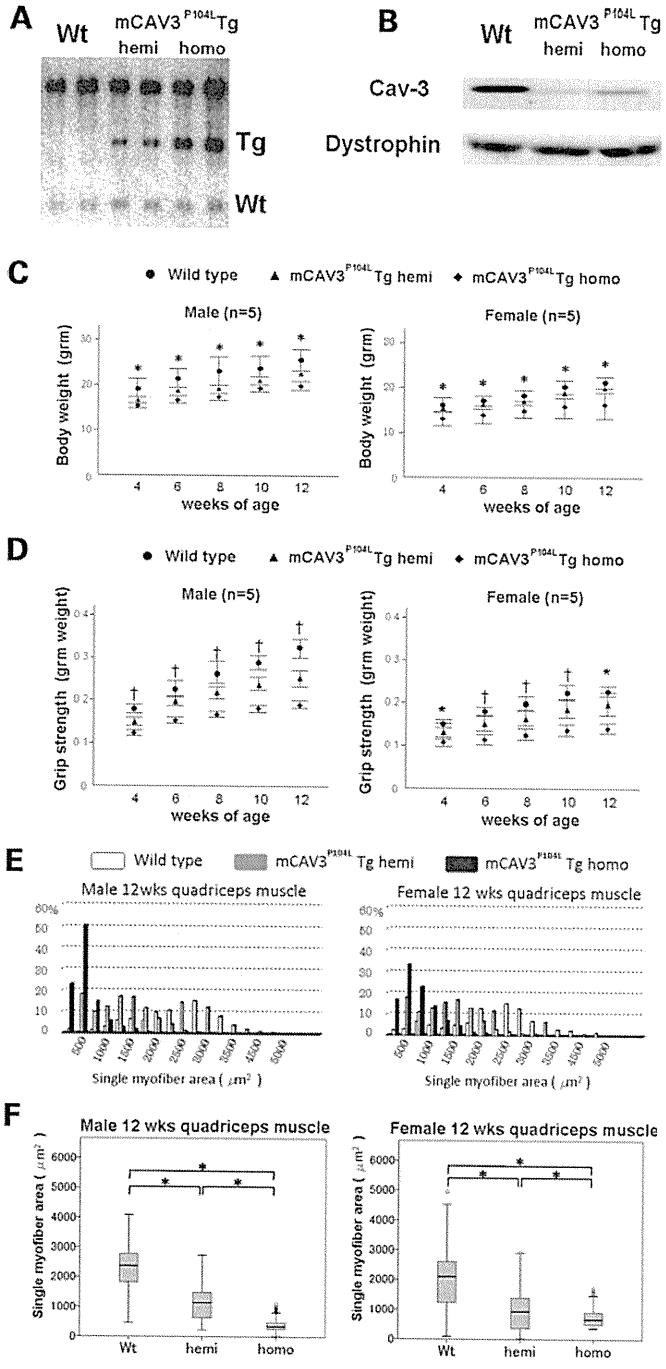

Figure 1. Effect of mCav3^{P104L} transgene dosage on the myopathic phenotype of LGMD1C model mice. (**A**) Genotyping of wild-type, hemizygous and homozygous transgenic mice by Southern blot analysis. A caveolin-3 DNA probe detected both endogenous caveolin-3 gene and mCav3^{P104L} transgene. Left to right, two independent samples of wild-type, hemizygous and homozygous transgenic mice. (**B**) Western blot analysis of caveolin-3 in skeletal muscles of wild-type and mCav3^{P104L} transgenic mice. Levels of caveolin-3 protein obviously decreased in the transgenic mice. Residual caveolin-3 was detected in homozygous mice. Temporal changes in body weight (**C**) and grip strength (**D**) of wild-type and transgenic mice between 4 and 12 weeks of age ($n = 5$ per group). Differences within each group were statistically determined using Scheffe's test. *Significant difference between wild-type and homozygous mice ($P < 0.05$). †Significant difference between each group ($P < 0.05$). Bars indicate standard error. (**E**) Histograms of individual myofiber areas in quadriceps muscle on transverse sections. Values were determined from 1000 myofibers per group. Bar = 100 μm. (**F**) Box plot represents non-parametric statistical analysis of myofiber areas of each group in (E). Significant difference between two groups (Mann–Whitney U test, $^*P < 0.005$).

We immunohistochemically analyzed cleaved caspase-3 and cytochrome *c* to further elucidate the ER stress response toward apoptosis in myofibers. Caspase-3 is activated by proteolysis in the signaling cascade toward apoptosis (20). Cleaved caspase-3, which is an active form of caspase-3, is increased in response not only to ER stress but also to

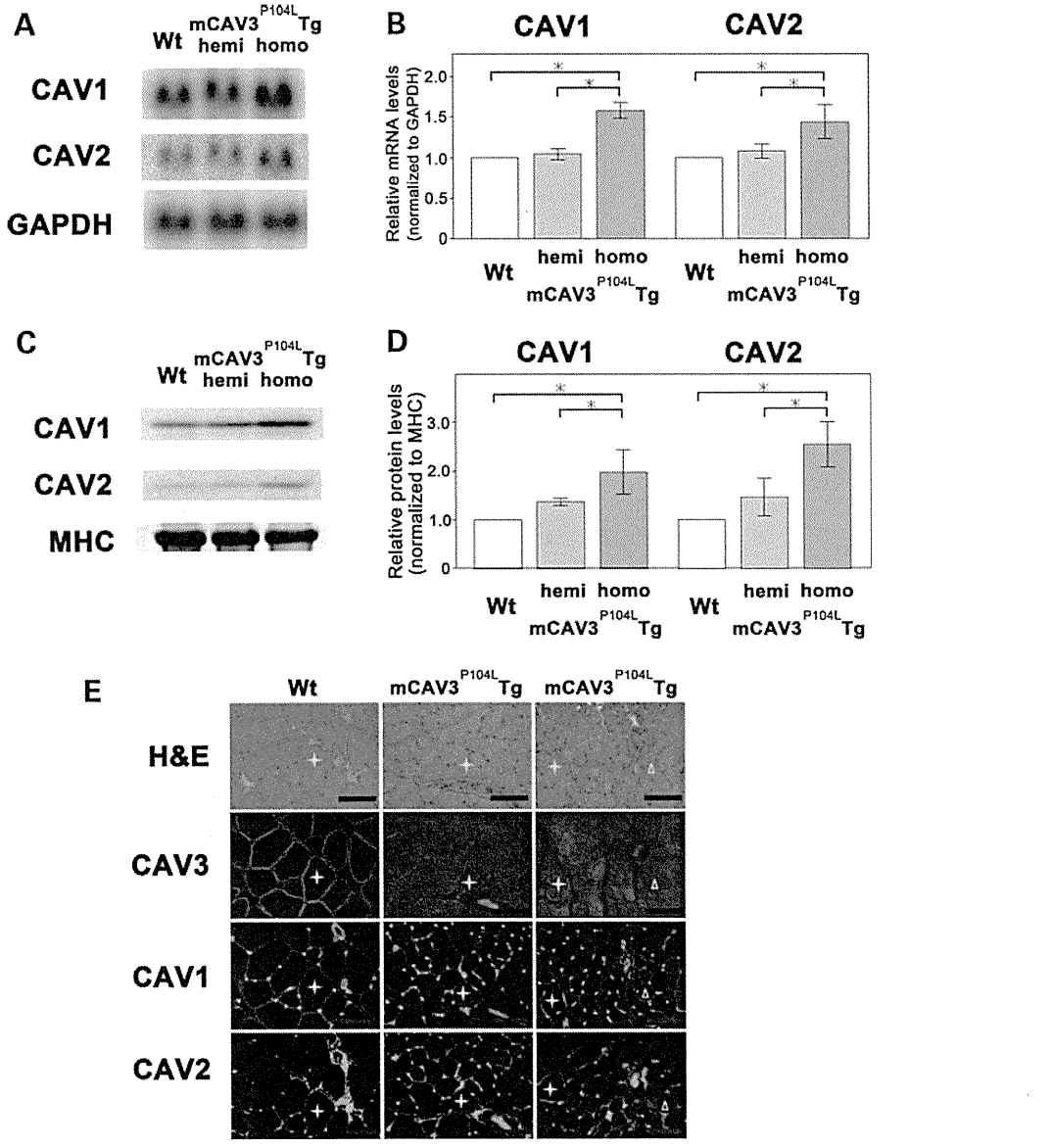

Figure 2. Expression of caveolin isoforms in mCav3^{P104L} transgenic mice. (**A**) Northern blot analysis. Upper panel, caveolin-1; middle panel, caveolin-2; lower panel, GAPDH as control. (**B**) Quantitative analysis of results from (A). (**C**) Western blot analysis. Upper panel, caveolin-1; middle panel, caveolin-2; lower panel, Coomassie blue-stained myosin heavy chain as standard control. (**D**) Quantitative analysis of results from (C). Signal intensity on blots determined from results of five independent experiments. Significant difference ($^*P < 0.05$) determined by Scheffe's test. (**E**) Immunohistochemical analysis of skeletal muscle cryosections from wild-type, hemizygous and homozygous transgenic mice. Crosses and triangles indicate identical myofibers on consecutive sections. H&E, hematoxylin and eosin staining. Caveolin isoforms, green; laminin, red.

apoptotic signals from the mitochondria (20,21). On the other hand, mitochondria specifically release cytochrome *c* into the cytosol under the latter conditions (20,22). Immunoreactivity for cleaved caspase-3 was obvious in the subsarcolemmal area of myofibers in mCav3^{P104L} transgenic mice (Fig. 5A). The average number of cleaved caspase-3 positive myofibers was increased in mCav3^{P104L} transgenic mice and differences between each genotype were significant (Fig. 5C). Cytochrome *c*-positive myofibers were rare in mCav3^{P104L} transgenic mice. Immunostained cleaved caspase-3 covered the entire area of myofibers that were frequently cytochrome *c*-positive in *mdx* and *dy*, but not in mCav3^{P104L} transgenic mice (Fig. 5A).

Apoptotic changes in myofibers were modest in mCav3^{P104L} transgenic mice compared with *mdx* or *dy* mice. We examined the expression of anti-apoptotic molecules from this perspective and found that *Dad1* mRNA was upregulated in mCav3^{P104L} transgenic mice (Fig. 6A and B). Dad1 is a subunit of the oligosaccharyl transferase complex that catalyzes the glycosylation of misfolded proteins to reduce ER stress (23,24). The upregulation of *Dad1* might contribute to the reduction of apoptosis in mCav3^{P104L} transgenic mice.

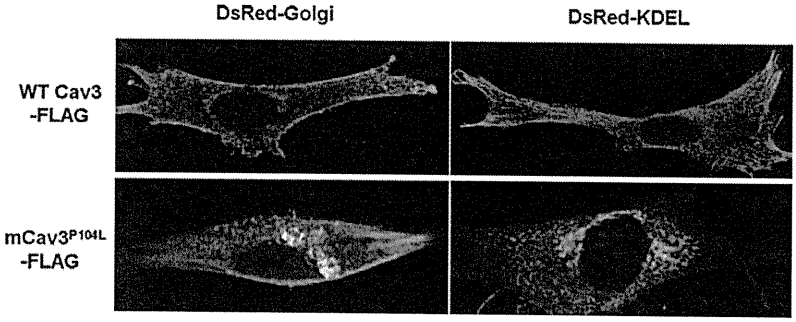

Figure 3. Immunostained C2C12 myoblasts transfected with wild-type or mCav3^{P104L} combined with a fluorescent marker that specifically localizes to ER or Golgi. Wild-type caveolin-3 (upper panels) and mCav3^{P104L} (lower panels) recognized by anti-FLAG tag antibody are shown in green. DsRed-Golgi marker (left panels) and DsRed-ER marker (right panels) recognized by anti-DsRed antibody are shown in red.

DISCUSSION

Mutations of the caveolin-3 gene cause LGMD with an autosomal dominant inheritance (6). Despite numerous studies *in vitro* using the disease-generating P104L mutant caveolin-3 (7–10), details of the molecular pathogenesis underlying LGMD1C have not been fully elucidated. Immunostaining for caveolin-3 at the sarcolemma is obviously lost in patients with LGMD1C (5,6). Galbiati's group proposed a dominant-negative effect of mutant caveolin-3 and demonstrated that it forms unstable aggregates of caveolin-3 hetero-oligomers with wild-type caveolin-3 that are retained in the Golgi complex (7) and that they are likely to be degraded by the ubiquitin–proteasome system (8). These data can explain why caveolin-3 protein levels were reduced in patients with LGMD1C. However, myopathy was notably milder in caveolin-3-null mice (25), but more severe in mCav3^{P104L} transgenic mice (13). Thus, a loss of caveolin-3 caused by the dominant-negative mechanism does not simply account for the severity of the disease in mice. A mechanism other than the reduced expression of caveolin-3 protein might function in the molecular pathogenesis of LGMD1C.

Here, we investigated phenotypic differences between hemizygous and homozygous mCAV3^{P104L} transgenic mice from morphological and molecular aspects. Myofiber hypotrophy and muscular weakness were more prominent in homozygous than in hemizygous mice. These findings indicated that the dosage of the mutant caveolin-3 transgene correlates with the severity of the myopathic phenotype. However, the lower level of residual caveolin-3 protein in hemizygous than in homozygous muscles is curious. This finding suggests that the level of mutant caveolin-3 determines the severity of myopathy through a toxic gain of function effect.

A unique feature of human LGMD1C is subsarcolemmal Golgi accumulation (possibly sarcoplasmic bodies) (5). The present and other studies have demonstrated mCav3^{P104L} accumulation in the Golgi apparatus *in vitro* (7,8,26). Previous pulse-chase experiments revealed that wild-type caveolin forms oligomers of about 400 kDa soon after the protein is synthesized in the ER (27). In addition, the mCav3^{P104L} proteins retained in the Golgi are composed of over 400 kDa high-molecular aggregates, and a proteasomal inhibitor causes such aggregates to accumulate within the ER (8). Together, newly synthesized mutant caveolin-3 protein could rapidly form misfolded aggregates in the ER, thereby inducing the ER stress response. Therefore, we analyzed the ER stress response to investigate a toxic gain of function effect of mCav3^{P104L}.

Indeed, we found that mCAV3^{P104L} induces the ER stress response in a gene-dose-dependent manner. Transcription of the molecular chaperone GRP78 was upregulated in mCav3^{P104L} transgenic mice. Under normal conditions, GRP78 suppresses the ER stress signaling pathway through direct interaction with ER stress transducers, such as PERK (16), which is a serine/threonine kinase that phosphorylates eIF2α (17,18). Misfolded proteins in the ER enlist GRP78 as a molecular chaperone. Once released from GRP78, the ER stress transducers trigger the cascade of gene regulation, known as the unfolded protein response (UPR). Molecular chaperones are commonly activated transcriptionally in the UPR (16). The phosphorylation of eIF2α by PERK is a crucial step in the UPR (17,18). We showed here that these molecular events occur in the skeletal muscle of mCav3^{P104L} transgenic mice, although PERK kinase activity was not directly demonstrated.

We also found that anti-apoptotic Dad1 (23,24) together with pro-apoptotic CHOP (18,19) is gene-dose dependently upregulated in mCAV3^{P104L} transgenic mice. This finding may be consistent with the limited numbers of TUNEL-positive myonuclei and cleaved caspase-3-positive myofibers in mCAV3^{P104L} transgenic mice compared with *mdx* or *dy* mice. Dystrophic changes such as necrotic/regenerating fibers or central nucleation are rarely observed and obvious myofiber hypotrophy is the most prominent feature of mCav3^{P104L} transgenic mice. Transgenic mice weigh less than wild-type mice by 4 weeks of age, which suggests the absence of normal hypertrophic growth or hypoplasia of the skeletal muscle. The most recent findings *in vitro* have revealed that the stable mCav3^{P104L} expression delays myoblast fusion (26). Therefore, the predominant small myofibers might be the result of impaired myotube formation rather than apoptosis. Overall, our results indicate that the apoptotic signaling in response to ER stress is counteracted by anti-apoptotic signaling in myofibers of mCav3^{P104L} transgenic mice, and that its contribution to myopathic change may be modest.

In conclusion, we demonstrated that mutant caveolin-3 dose-dependently induces the ER stress response, which would be a toxic gain of function effect related to the pathophysiology of LGMD1C.

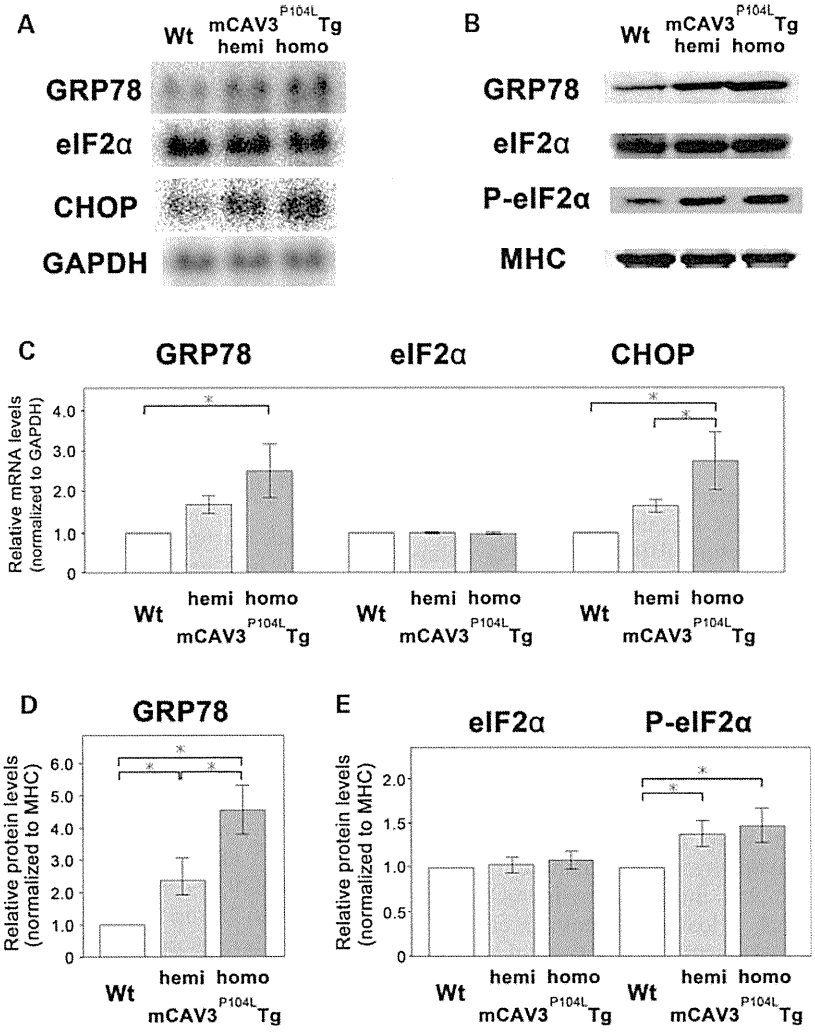

Figure 4. Endoplasmic reticulum stress response in mCav3^{P104L} transgenic mice. (**A**) Northern blot analysis of skeletal muscle from each group. Upper to lower panels, mRNA levels of GRP78, CHOP, eIF2α and GAPDH. (**B**) Western blot analysis of skeletal muscle from each group. Upper to lower panels, protein levels of GRP78, eIF2α and phosphorylated-eIF2α. Control Coomassie blue-stained myosin heavy chain. (**C**) Quantitative analysis of results from (A). (**D**) Quantitative analysis of GRP78 expression based on results from (B). Signal intensity on blots determined from results of five independent experiments. *Significant difference determined by Scheffe's test ($P < 0.05$).

MATERIALS AND METHODS

Animals

Mice were aged about 12 weeks in this study. The construct for the generation of mCav3^{P104L} transgenic mice has been described (13,14). All animal experiments proceeded at the Laboratory Animal Center under the approval of the Animal Research Committee of Kawasaki Medical School.

Muscle morphology and immunohistochemistry

Unfixed distal hindlimb muscles were snap-frozen in liquid nitrogen-cooled isopentane and sectioned transversely (10 μm) at the center of tibialis anterior (or quadriceps) muscle using a cryostat (Leica Microsystems). Sections were post-fixed in cold methanol for 10 min, and then immunostained using the Mouse on Mouse Kit (Vector Laboratories) according to the manufacturer's recommendations. The primary antibodies were as follows: rabbit polyclonal anti-caveolin-1 (BD Transduction Laboratories), mouse monoclonal anti-caveolin-2 (BD Transduction Laboratories), rabbit polyclonal anti-caveolin-3 (Alexis Corporation), rabbit polyclonal anti-cleaved caspase-3 (Cell Signaling Technology), anti cytochrome *c* (eBioscience) and rat monoclonal anti-laminin α2 (Alexis Corporation). Secondary antibodies were conjugated with fluorescein isothiocyanate.

Cell staining

C2C12 and COS7 cells were cultured on coverslips treated with the FuGENE6 transfection reagent (Roche) and then cotransfected with a caveolin-3-FLAG vector or an

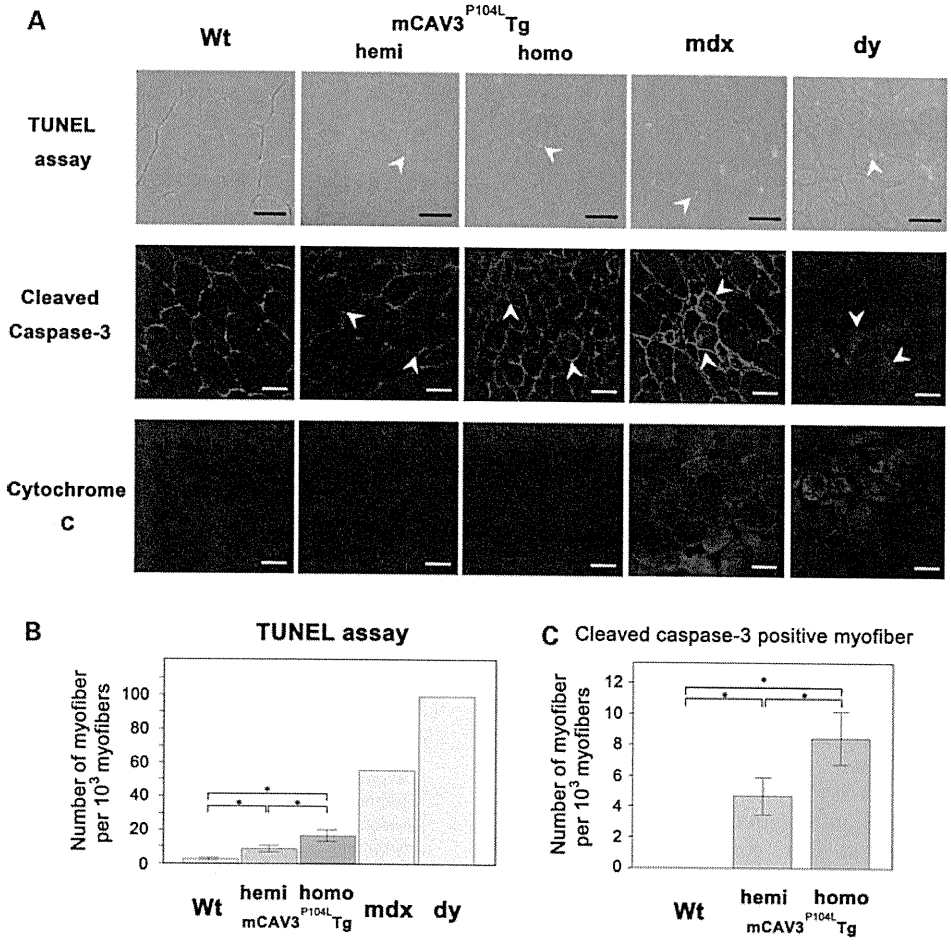

Figure 5. (**A**) (Upper panels) Typical appearance of apoptotic nuclei detected by TUNEL assays in mouse models of muscular dystrophy. Arrowheads indicate TUNEL-positive nuclei inside myofibers. (Middle and lower) Immunohistochemical analysis of skeletal muscle cryosections from mouse models of muscular dystrophy. (Middle panels) Cleaved caspase-3, red; laminin, green; DAPI, blue. Arrowheads indicate myofibers with immunoreactivity for cleaved caspase-3. (Lower panels) Cytochrome *c*, green. Bar = 50 μm (**B**) Numbers of myofibers with TUNEL-positive nuclei calculated per 1000 myofibers from independent samples ($n = 4$ per group of mutant caveolin-3 transgenic mice; positive control *mdx* and *dy* mice; $n = 2$ per group). Significant difference determined by Scheffe's test ($^*P < 0.05$). (**C**) Numbers of myofibers that were immunoreactive for cleaved caspase-3 per 1000 myofibers ($n = 3$ per group of mutant caveolin-3 transgenic mice). Significant difference determined by Scheffe's test ($^*P < 0.05$).

mCav3^{P104L} vector and pDsRed-Golgi (Clontech) or pCS2-DsRed-KDEL (a gift from Dr S. Nishimatsu). Twelve hours later, the cells were fixed in phosphate-buffered saline (PBS) containing 4% paraformaldehyde for 15 min and then permeabilized with PBS containing 0.5% Triton X-100 for 15 min. Non-specific binding was blocked with 3% bovine serum albumin in PBS containing 0.5% Triton X-100 for 1 h at room temperature. Cells were incubated with an anti-FLAG antibody (Sigma) and an anti-DsRed antibody (Clontech) at 4°C, followed by a secondary antibody.

TUNEL assay

Cryosections of quadriceps muscles (10 μm) were fixed with 1% paraformaldehyde in PBS for 10 min at room temperature. The sections were then post-fixed in ethanol:acetic acid (2:1) for 5 min at −20°C, labeled with digoxigenin-conjugated dNTP via the enzymatic activity of terminal deoxynucleotidyl transferase and reacted with anti-digoxigenin fluorescein antibody according to the manufacturer's recommendations (Chemicon). TUNEL-positive nuclei were counted in photographs of 15 sections from each sample.

RT-PCR

We reverse-transcribed cDNA templates from RNAs extracted from C2C12 cells. Genes were amplified using the following respective forward and reverse primers: caveolin-1, 5′-GACTGCCAAGCCTGTTGTAA-3′ and 5′-CAAACTGTG GCCATGCCAG-3′; caveolin-2, 5′-CATAAGGCTAGCTAG AGGCA-3′ and 5′-GGAGAGAACACCTAGACAGC-3′; GRP78, 5′CTTCGAAGGAGAAGACTTCTC-3′ and 5′-CTG TACCTTTGTCTTCAGCTG-3′; eIF2α, 5′-ATCTAATAGC TCCACCCAGG-3′ and 5′-AACAGCTGACATGA AGGAGG-3′; CHOP, 5′-CTGCCTTTCACCTTGGAGAC-3′ and 5′-GCTCGATTTCCTGCTTGAGC-3′; GAPDH, 5′-CGT AGACAAAATGGTGAAGG-3′ and 5′-GTTGTCATGGA TGACCTTGG-3′.

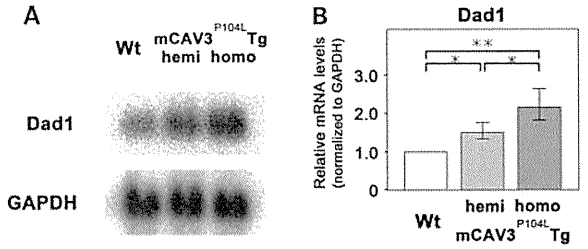

Figure 6. Upregulation of an anti-apoptotic molecule, Dad1, in mCav3^{P104L} transgenic mice. (**A**) Northern blot analysis of Dad1 in skeletal muscle from wild-type, hemizygous and homozygous transgenic mice. (**B**) Quantitative analysis of results from (A). Signal intensity on blots determined from results of five independent experiments. Significant difference determined by Scheffe's test ($^*P < 0.05$).

Northern blot analysis

The RT-PCR products of mouse cDNAs were subcloned into pCRII-TOPO (Invitrogen) and then digested with EcoRI. The digest was separated by agarose gel electrophoresis and extracted using the Rapid Gel Extraction System (Marligen Bioscience). Fragments of DNA were then labeled with [α-^{32}P]-dCTP using the MegaPrime DNA Labeling System (GE Healthcare) and RNAs were extracted from the skeletal muscles of mice in each genotype group. Total RNA (20 μg) was separated on 0.9% agarose gels containing 7% formaldehyde and blotted onto Hybond-N$^+$ (GE Healthcare). Hybridization proceeded at 42°C for 24 h, and then bands were visualized by autoradiography using Fuji Imaging Plates (Fujifilm). All northern blot experiments were repeated at least three times using different sets of samples.

Western blot analysis

Mouse skeletal muscles were homogenized in 10 volumes (w/v) of a buffer comprising 50 mM Tris–HCl (pH 7.4), 100 mM NaCl, 1 mM EDTA, 5 mM β-mercaptoethanol, 0.1 mM PMSF and 1 mM benzamidine. Crude muscle homogenates were separated by SDS-PAGE (3–20% linear acrylamide gradient) and transferred to polyvinylidene difluoride membranes. Antibodies were purchased from the indicated sources: goat polyclonal anti-GRP78 (Santa Cruz Biotechnology), mouse monoclonal anti-eIF2α (Abcam), rabbit polyclonal anti-Ser51 phosphorylated eIF2α (Abcam), rabbit polyclonal anti-caveolin-1 (BD Transduction Laboratories), mouse monoclonal anti-caveolin-2 (BD Transduction Laboratories) and rabbit polyclonal anti-caveolin-3 (Alexis Corporation). All western blot experiments were repeated at least five times, with different sets of samples. Immunoblot band intensities were standardized with Coomassie blue staining of myosin heavy chain in each sample and analyzed using Multi Gauge version 2.2 software (Fujifilm).

SUPPLEMENTARY MATERIAL

Supplementary Material is available at *HMG* online.

ACKNOWLEDGEMENTS

We thank M. Fujino (postgraduate student, Kawasaki Welfare School), A. Mimura, N. Oka and K. Yamane (Kawasaki Medical School), as well as N. Naoe and T. Kenmotsu (Department of Neurology, Kawasaki Medical School) for excellent technical assistance.

Conflict of Interest statement. None declared.

FUNDING

This study was supported by JSPS KAKENHI 20591013 and 21591101, a research grant for Nervous and Mental Disorders from the Ministry of Health, Labour and Welfare of Japan (20B-13), by grants for Research on Psychiatric and Neurological Diseases and Mental Health from the Ministry of Health, Labour and Welfare of Japan (H20-016, H20-018) and by research project grants from the Kawasaki Medical School (20-604, 21-602 and 22-T1).

REFERENCES

1. Richter, T., Floetenmeyer, M., Ferguson, C., Galea, J., Goh, J., Lindsay, M.R., Morgan, G.P., Marsh, B.J. and Parton, R.G. (2008) High-resolution 3D quantitative analysis of caveolar ultrastructure and caveola-cytoskeleton interactions. *Traffic*, **9**, 893–909.
2. Rothberg, K.G., Heuser, J.E., Donzell, W.C., Ying, Y., Glenney, J.R. and Anderson, R.G.W. (1992) Caveolin, a protein component of caveolae membrane coats. *Cell*, **68**, 673–682.
3. Song, K.S., Scherer, P.E., Tang, Z., Okamoto, T., Li, S., Chafel, M., Chu, C., Kohtz, D.S. and Lisanti, M.P. (1996) Expression of caveolin-3 in skeletal, cardiac, and smooth muscle cells. *J. Biol. Chem.*, **271**, 15160–15165.
4. Woodman, S.E., Sotgia, F., Galbiati, F., Minetti, C. and Lisanti, M.P. (2004) Caveolinopathies: mutations in caveolin-3 cause four distinct autosomal dominant muscle diseases. *Neurology*, **62**, 538–543.
5. Fulizio, L., Nascimbeni, A.C., Fanin, M., Piluso, G., Politano, L., Nigro, V. and Angelini, C. (2005) Molecular and muscle pathology in a series of caveolinopathy patients. *Hum. Mutat.*, **25**, 82–89.
6. Minetti, C., Sotgia, F., Bruno, C., Scartezzini, P., Broda, P., Bado, M., Masetti, E., Mazzocco, M., Egeo, A., Donati, M.A. *et al.* (1998) Mutations in the caveolin-3 gene cause autosomal dominant limb-girdle muscular dystrophy. *Nat. Genet.*, **18**, 365–368.
7. Galbiati, F., Volonté, D., Minetti, C., Chu, J.B. and Lisanti, M.P. (1999) Phenotypic behavior of caveolin-3 mutations that cause autosomal dominant limb girdle muscular dystrophy (LGMD-1C). *J. Biol. Chem.*, **274**, 25632–25641.
8. Galbiati, F., Volonté, D., Minetti, C., Bregman, D.B. and Lisanti, M.P. (2000) Limb-girdle muscular dystrophy (LGMD-1C) mutants of caveolin-3 undergo ubiquitination and proteasomal degradation. *J. Biol. Chem.*, **275**, 37702–37711.
9. Galbiati, F., Volonté, D., Engelman, J.A., Scherer, P.E. and Lisanti, M.P. (1999) Targeted down-regulation of caveolin-3 is sufficient to inhibit myotube formation in differentiating C2C12 myoblasts. *J. Biol. Chem.*, **274**, 30315–30321.
10. Fanzani, A., Stoppani, E., Gualandi, L., Giuliani, R., Galbiati, F., Rossi, S., Fra, A., Preti, A. and Marchesini, S. (2007) Phenotypic behavior of C2C12 myoblasts upon expression of the dystrophy-related caveolin-3 P104L and TFT mutants. *FEBS Lett.*, **581**, 5099–5104.
11. Conway, K.A., Harper, J.D. and Lansbury, P.T. (1998) Accelerated in vitro fibril formation by a mutant alpha-synuclein linked to early-onset Parkinson disease. *Nat. Med.*, **4**, 1318–1320.
12. Xiong, H., Wang, D., Chen, L., Choo, Y.S., Ma, H., Tang, C., Xia, K., Jiang, W., Ronai, Z., Zhuang, X. *et al.* (2009) Parkin, PINK1, and DJ-1 form a ubiquitin E3 ligase complex promoting unfolded protein degradation. *J. Clin. Invest.*, **119**, 650–660.

13. Sunada, Y., Ohi, H., Hase, A., Ohi, H., Hosono, T., Arata, S., Higuchi, S., Matsumura, K. and Shimizu, T. (2001) Transgenic mice expressing mutant caveolin-3 show severe myopathy associated with increased nNOS activity. *Hum. Mol. Genet.*, **10**, 173–178.
14. Ohsawa, Y., Toko, H., Katsura, M., Morimoto, K., Yamada, H., Ichikawa, Y., Murakami, T., Ohkuma, S., Komuro, I. and Sunada, Y. (2004) Overexpression of P104L mutant caveolin-3 in mice develops hypertrophic cardiomyopathy with enhanced contractility in association with increased endothelial nitric oxide synthase activity. *Hum. Mol. Genet.*, **13**, 151–157.
15. Ohsawa, Y., Hagiwara, H., Nakatani, M., Yasue, A., Moriyama, K., Murakami, T., Tsuchida, K., Noji, S. and Sunada, Y. (2006) Muscular atrophy of caveolin-3-deficient mice is rescued by myostatin inhibition. *J. Clin. Invest.*, **116**, 2924–2934.
16. Ni, M. and Lee, A.S. (2007) ER chaperones in mammalian development and human diseases. *FEBS Lett.*, **581**, 3641–3651.
17. Harding, H.P., Zhang, Y., Bertolotti, A., Zeng, H. and Ron, D. (2000) PERK is essential for translational regulation and cell survival during the unfolded protein response. *Mol. Cell*, **5**, 897–904.
18. Harding, H.P., Novoa, I., Zhang, Y., Zeng, H., Wek, R., Schapira, M. and Ron, D. (2000) Regulated translation initiation controls stress-induced gene expression in mammalian cells. *Mol. Cell*, **6**, 1099–1108.
19. Oyadomari, S. and Mori, M. (2004) Roles of CHOP/GADD153 in endoplasmic reticulum stress. *Cell Death Differ.*, **11**, 381–389.
20. Li, P., Nijhawan, D., Budihardjo, I., Srinivasula, S.M., Ahmad, M., Alnemri, E.S. and Wang, X. (1997) Cytochrome c and dATP-dependent formation of Apaf-1/caspase-9 complex initiates an apoptotic protease complex. *Cell*, **91**, 479–489.
21. Morishima, N., Nakanishi, K., Takenouchi, H., Shibata, T. and Yasuhiko, Y. (2002) An endoplasmic reticulum stress-specific caspase cascade in apoptosis. *J. Biol. Chem.*, **277**, 34287–34294.
22. Kluck, R.M., Bossy-Wetzel, E., Green, D.R. and Newmeyer, D.D. (1997) The release of cytochrome c from mitochondria. *Science*, **275**, 1132–1136.
23. Kelleher, D.J. and Gilmore, R. (1997) DAD1, the defender against apoptotic cell death, is a subunit of the mammalian oligosaccharyltransferase. *Proc. Natl. Acad. Sci. USA*, **94**, 4994–4999.
24. Kelleher, D.J. and Gilmore, R. (2006) An evolving view of the eukaryotic oligosaccharyltransferase. *Glycobiology*, **16**, 47R–62R.
25. Hagiwara, Y., Sasaoka, T., Araishi, K., Imamura, M., Yorifuji, H., Nonaka, I., Ozawa, E. and Kikuchi, T. (2000) Caveolin-3 deficiency causes muscle degeneration in mice. *Hum. Mol. Genet.*, **9**, 3047–3054.
26. Stoppani, E., Rossi, S., Meacci, E., Penna, F., Costelli, P., Bellucci, A., Faggi, F., Maiolo, D., Monti, E. and Fanzani, A. (2011) Point mutated caveolin-3 form (P104L) impairs myoblast differentiation via Akt and p38 signalling reduction, leading to an immature cell signature. *Biochim. Biophys. Acta*, **1812**, 468–479.
27. Monier, S., Parton, R.G., Vogel, F., Behlke, J., Henske, A. and Kurzchalia, T.V. (1995) VIP21-caveolin, a membrane protein constituent of the caveolar coat, oligomerizes in vivo and in vitro. *Mol. Biol. Cell*, **6**, 911–927.

Journal of Human Genetics (2011) 56, 330–334

www.nature.com/jhg

ORIGINAL ARTICLE

Genetic and clinical analysis in a Chinese parkinsonism-predominant spinocerebellar ataxia type 2 family

Hao Sun[1], Wataru Satake[2], Changjun Zhang[3], Yoshitaka Nagai[2], Youyong Tian[4], Shouzhi Fu[4], Jiankun Yu[1], Yaping Qian[1], Yuan Qian[1], Jiayou Chu[1] and Tatsushi Toda[2]

Parkinson's disease is a degenerative central nervous system disorder that often impairs motor skills, speech and other functions. We discovered a large Chinese family showing primarily parkinsonism symptoms with autosomal dominant inheritance. Six affected individuals in the family showed typical parkinsonism symptoms, including pill-rolling tremor. Two other affected individuals showed cerebellar ataxia symptoms. A whole-genome scan using the 50K single nucleotide polymorphism array with three different linkage methods detected two positive regions on chromosome 12q24.1 and 5q13.3. The *ATXN2* gene, responsible for spinocerebellar ataxia type 2 (SCA2) was located precisely in the center of the positive region on chromosome 12. Further analysis of SCA2 revealed heterozygous pathological CAG expansions in the family. The affected individuals' symptoms were typical of parkinsonism, but complex. Inverse correlation between CAG repeat size and age of onset is not obvious in this pedigree. This parkinsonism-predominant SCA2 family shared the same disease gene locus with other 'standard' SCA2 families, but it is possible that variations in one or more modifier genes might account for the parkinsonism-predominant SCA2 predisposition observed in this pedigree.
Journal of Human Genetics (2011) **56**, 330–334; doi:10.1038/jhg.2011.14; published online 10 February 2011

Keywords: 5q13; genome-wide scan; linkage study; single nucleotide polymorphism chip

INTRODUCTION

Parkinson's disease (PD), a degenerative central nervous system disorder, often impairs motor skills, speech and other functions.[1] It is found worldwide, with incidence rates varying from country to country. The prevalence of PD increases with age. In Europe, PD affects about 1–2% of individuals over 60 years of age.[2] Although there is no cure for PD, further understanding of its genetic risks can improve neuroprotective or preventive approaches. Causative genes for Mendelian-inherited parkinsonism have been identified. Point mutations and multiplications in the *SNCA* gene have been found in some families with autosomal dominant inheritance.[3,4] To date, mutations in the *LRRK2* gene are the most common cause of Mendelian PD. In studies across several populations, 5–15% of autosomal dominant PD families carried mutations in *LRRK2* (see refs 5, 6). Mutations in three genes, *PARK2* (encoding parkin), *PINK1* (*PARK6*) and *DJ-1* (*PARK7*), have been identified in autosomal recessive PD, which is characterized by an early age at onset and therefore referred to as autosomal recessive juvenile parkinsonism.[7–9] The expanded *ATXN2* gene, which causes spinocerebellar ataxia type 2 (SCA2), was found in some families with only or mainly typical parkinsonism.[10,11] Although some parkinsonism clinical signs such as dystonia and tremor have been described in SCA2, dopamine-responsive parkinsonism has been infrequently described in SCA2 (see ref. 12). The sign of dopamine-responsive just has been seen in some Chinese families[13,14] and some white families.[15,16]

We described here a large family from Hubei, China, that showed primarily autosomal dominant inheritance of parkinsonism symptoms acrossing four generations. Affected family members exhibited typical clinical features of PD, such as pill-rolling tremors and levodopa responsiveness. However, some family members showed cerebellar symptoms. The patients who showed the atypical phenotypes opposed to the typical cerebellar ataxia maybe have more complex genetic causes than normal SCA2 patients. So, we performed a whole-genome linkage study to identify possible genetic causes in

[1]The Department of Medical Genetics, Institute of Medical Biology, Chinese Academy of Medical Sciences and Peking Union Medical College, Yunnan, China; [2]Division of Neurology/Molecular Brain Science, Kobe University Graduate School of Medicine, Kobe, Japan; [3]Institute of Eugenics and Genetics, Hubei, China and [4]Emergency Department, the Peoples Hospital of Shiyan, Hubei, China
Correspondence: Professor T Toda, Division of Neurology/Molecular Brain Science, Kobe University Graduate School of Medicine, 7-5-1 Kusunoki-chou, Chuo-ku, Kobe 650-0017, Japan.
E-mail: toda@med.kobe-u.ac.jp
or Professor J Chu, The Department of Medical Genetics, Institute of Medical Biology, Chinese Academy of Medical Sciences and Peking Union Medical College, 379 Jiaolin Road, Kunming, Yunnan 650118, China.
E-mail: chujy@imbcams.com.cn
Received 29 November 2010; revised 10 January 2011; accepted 13 January 2011; published online 10 February 2011

this family. At same time, the molecular and clinical features of this family were analyzed.

MATERIALS AND METHODS

Clinical information

The proband (IV-3) was initially diagnosed as PD in 2001, and therefore the family was classified as a PD pedigree. In 2007, we performed neurological examinations for eight patients in the family, and we examined four patients using magnetic resonance imaging (MRI). Blood samples were obtained from patients and unaffected relatives with informed consent. Approval for the study was obtained from the Ethical Committees of participating institutions.

Whole-genome linkage analysis

Genomic DNA was isolated from blood using QIAamp DNA Blood Mini Kits (Qiagen, Shanghai, China). Single nucleotide polymorphism genotyping was performed for 27 individuals from the family (Figure 1) using the Human Mapping 50K Xba 240 SNP array (Affymetrix, Santa Clara, CA, USA). Signal intensity data were analyzed using GeneChip DNA analysis software GDAS v.3.0.2.8 (Affymetrix). The genotype data were converted to linkage format using ALOHOMORA software[17] and subjected to quality control routines, including gender check and graphical representation of relationship errors.[18] Mendelian errors were detected with PedCheck,[19] and non-informative markers were deleted before further analysis. Genome-wide non-parametric multipoint linkage, single parametric and single non-parametric linkage analysis were performed using GeneSpring GT software (Agilent, Santa Clara, CA, USA).

Trinucleotide repeat analysis

We screened for mutations in the *ATXN2* gene using PCR amplification with previously published SCA-2A and SCA-2B oligonucleotide primers.[20] PCR products were sized precisely using capillary electrophoresis with an ABI 3730xL DNA analyzer (Applied Biosystems, Foster city, CA, USA) and compared with known samples using GeneMapper V3.5 (Applied Biosystems, Foster city, CA, USA). Some samples were isolated from agarose gels and used as DNA templates for sequencing with the Big-dye terminator kit (Applied Biosystems) on the ABI 3730xL analyzer.

RESULTS

Clinical information

The family (Figure 1) consisted of 39 members in four generations, with 16 affected members. All family members reside in Hubei Province, China. The inheritance pattern is autosomal dominant. We collected peripheral blood from 27 family members, including 10 affected members. Clinical data were shown in Table 1 for 8 of 10 patients collected in 2007. Detailed clinical data were unavailable for

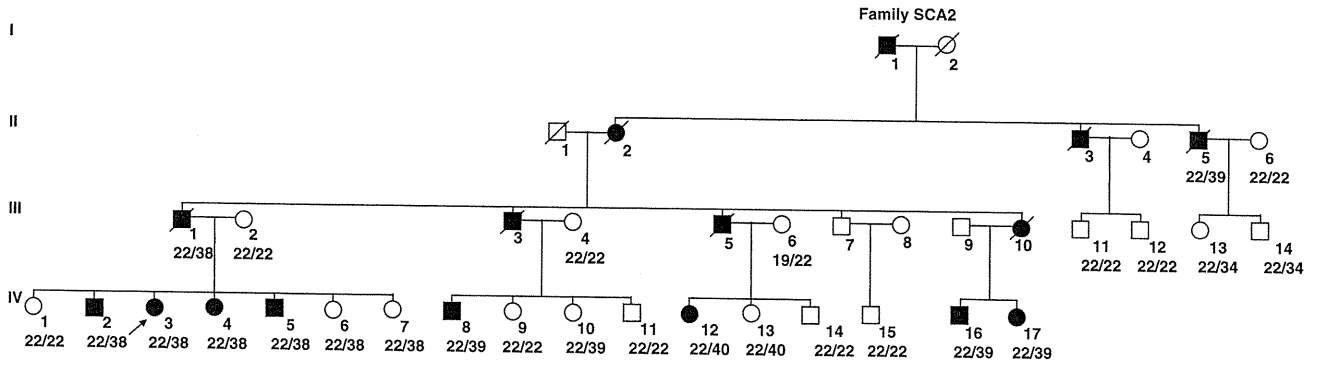

Figure 1 Pedigree of a Chinese family ascertained with parkinsonism-predominant spinocerebellar ataxia type 2 (SCA2). Squares indicate males; circles, females. A slash through the symbol indicates deceased and an arrow points to the proband. The pedigree contains 16 known affected individuals; eight patients are living. SCA2 CAG repeat allele sizes are listed below the pedigree symbols of the 27 individuals who have been genotyped.

Table 1 Clinical and genetic features of the SCA2 family

No.	*IV-2*	*IV-3*	*IV-4*	*IV-5*	*IV-8*	*IV-12*	*IV-16*	*IV-17*
Age at onset	33	36	37	22	20	37	39	35
Age at examination	46	44	42	39	50	45	51	38
Resting tremor	2	1	0	2	0	0	2[a]	0
Bradykinesia	3	2	0	3	0	1	2	2
Rigidity	3	2	0	2	0	1	2	1
Postural instability	2	1	0	2	0	2	2	1
Masked face	3	2	0	3	1	2	2	2
Levodopa response	+	+	–	NT	NT	+	+	NT
Gait ataxia	0	0	2	1	0	0	0	0
Limb ataxia	1	1	2	1	0	0	0	0
Slow saccade	2	1	1	2	3[b]	1	1	0
Vertical gaze palsy	2	0	0	2	3[b]	0	0	0
Hyporeflexia	3	3	1	0	1	0	0	0
Cerebellar atrophy on MRI	2	1	3	1	NT	NT	NT	NT
CAG repeats	22/38	22/38	22/38	22/38	22/39	22/40	22/39	22/39

Abbreviations: MRI, magnetic resonance imaging; SCA2, spinocerebellar ataxia type 2.
[a]Pill-rolling tremor.
[b]difficulty initiating pursuit movements.
0 indicates that the individual was tested and the symptom was absent. 1, mild; 2, moderate; and 3, marked. NT indicates that the individual could not be tested. A (+) indicates that the finding was present; a (–) indicates absent.

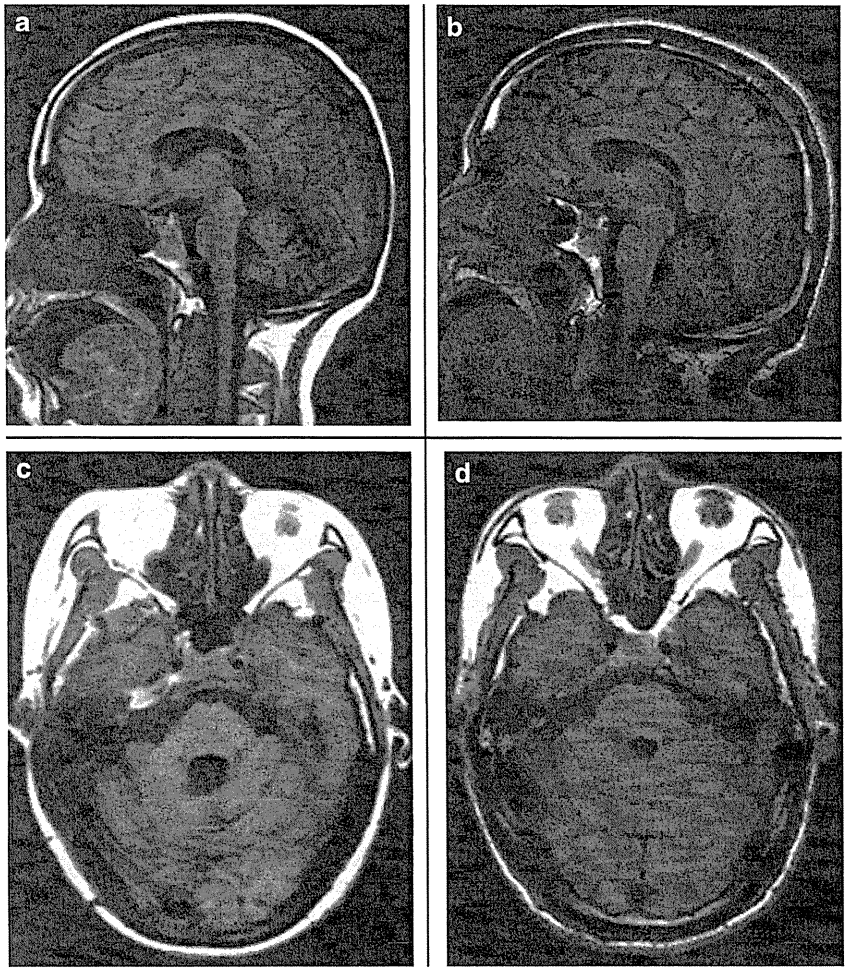

Figure 2 T1-weighted magnetic resonance imaging (MRI) of IV-4 (**a**, **c**) and IV-5 (**b**, **d**). Patient IV-4 showed marked cerebellar atrophy, and patient IV-5 showed no cerebellar atrophy.

the other two deceased patients (II-5 and III-1). Family members of the two patients provided ambiguous clinical data, and their preliminary diagnosis indicated that the two patients had parkinsonism symptoms. Blood samples, collected in 2001, were provided by their neurologist. Age of symptomatic disease onset varied from 20 to 39 years, with an average age at onset of 32.4 years.

Most patients showed typical parkinsonism symptoms, such as resting tremor, bradykinesia, rigidity and postural instability (IV-2, IV-3, IV-5, IV-12, IV-16 and IV-17). Patient IV-16 had pill-rolling tremors. However, two patients (IV-4 and IV-8) showed cerebellar symptoms such as limb ataxia and slow saccade, but no typical parkinsonism symptoms.

Five of eight patients were treated with levodopa. Only one (Patient IV-4) of them showed no response. This patient also lacked typical parkinsonism symptoms. Patients IV-2, IV-3, IV-4 and IV-5 were examined using MRI analysis. MRI images from Patients IV-4 and IV-5 were shown in Figure 2. Marked cerebellar atrophy was found in Patient IV-4, and no cerebellar atrophy was found in Patient IV-5.

Whole-genome linkage analysis

Genome-wide analysis revealed two positive regions for linkage, on chromosomes 12 and 5. On chromosome 12, the highest single-point parametric log of odds (LOD) score (2.59) was detected at rs2695281 (100.5 Mb, NCBI Build 36). The highest multi-point non-parametric LOD score on chromosome 12 was 3.5, with a multi-point non-parametric LOD score >3 at 94.9–115.6 Mb (NCBI Build 36). On chromosome 5, the highest single-point parametric LOD score (2.73) was detected at rs10491487 (80.4 Mb, NCBI Build 36). The highest multi-point non-parametric LOD score on chromosome 5 was 3.5 with a multi-point non-parametric LOD score >3 at 79.8–81.2 Mb (NCBI Build 36). Multi-point non-parametric linkage results were compatible with the single-point parametric linkage results on both chromosomes 5 and 12. Single-point non-parametric linkage analysis detected no positive result. Most of single-point non-parametric LOD scores were smaller than 2, and the highest was 2.1, on chromosome 21 (Figure 3). Gender and relationships in the single nucleotide polymorphism array data were accurate, and PedCheck detected no Mendelian errors.

The *ATXN2* gene, responsible for SCA2, was located at 110.3 Mb (NCBI Build 36) on chromosome 12, within the linkage-positive region of 94.9–115.6 Mb.

Trinucleotide repeat analysis

We performed SCA2 molecular analysis in all 27 family members. Three types of heterozygous pathological CAG expansion (38, 39 and 40 repeats) and two types of normal repeats (19 and 22) were identified. A borderline 34 CAG repeat was found in the two family members. Genotyopes with repeat numbers for individual family

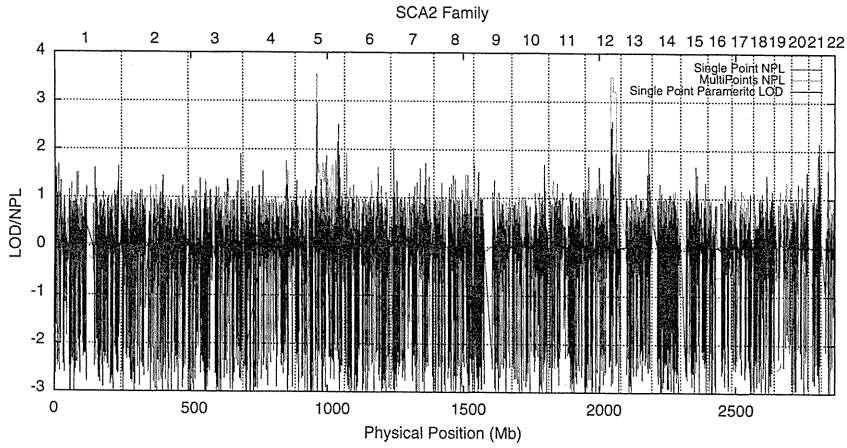

Figure 3 Three types of log of odds (LOD) scores were calculated from the genome-wide scan. The LOD score plot was created with GNUPLOT 4.0 (http://www.gnuplot.info) using the LOD plot-drawing Perl script included in the ALOHOMORA package. On chromosome 12, the highest MultiPoint non-parametric LOD score was 3.5 and the highest SinglePoint parametric LOD score was 2.59. On chromosome 5, the highest MultiPoint non-parametric LOD score was 3.5 and the highest SinglePoint parametric LOD score was 2.73. The MultiPoint non-parametric linkage results were compatible with the SinglePoint parametric linkage results on chromosomes 5 and 12. LOD scores <-3 are not shown.

members were shown in Figure 1. Sequence analysis of expanded alleles from IV-5, IV-8, IV-12 and III-14 revealed interruptions of CAG base pair repeats with CAA. The 38-repeat expansion in IV-5 contained 29 CAGs, followed by one CAA and eight CAGs. The 39-repeat expansion IV-8 contained 30 CAGs, one CAA and eight CAGs. The 40-repeat expansion in IV-12 contained 31 CAGs, one CAA and eight CAGs. The normal 34-repeat CAG expansion in III-14 contained 25 CAGs, one CAA and eight CAGs.

All affected individuals in the branch of III-1 carried 38 trinucleotide repeats. IV-6 and IV-7 also carried the 38 trinucleotide repeats, but as of 2007 no parkinsonism or ataxia had been observed in these individuals. The 39 trinucleotide repeats occurred in the branches of II-5, III-3 and III-10. Similar to IV-6 and IV-7, individual IV-10 carried the 39 trinucleotide repeats, but had shown no parkinsonism or ataxia symptoms in 2007. In the branch of II-5, the 39 repeats were shortened to 34 in transmission. III-13 and III-14, who carried 34 trinucleotide repeats, showed no symptoms.

DISCUSSION

We described a levodopa-responsive parkinsonism Chinese family with SCA2 trinucleotide expansions. The symptoms observed in this family were primarily parkinsonism, but complex. Some affected family members showed typical clinical manifestations of parkinsonism. Four of five patients responded to levodopa treatment. One affected individual (IV-4) lacking parkinsonism symptoms was unresponsive to levodopa; MRI analysis of this patient showed marked cerebellar atrophy. Patient IV-8 showed just mild masked face, but his cerebellar symptoms were severe. In other patients (IV-12, IV-16 and IV-17), cerebellar symptoms were minor or absent. Overall, the clinical signs in this family appear most similar to parkinsonism.

Molecular analysis of SCA2 expansion in the family revealed three types of expanded CAG repeats. An inverse correlation has been established between age of SCA2 onset and CAG repeat length, with repeat length accounting for 54–80% of variance.[21,22] However, such inverse correlation was not observed in our pedigree. In the branches of III-1 and III-2, the age of onset in affected individuals who carried the 38 CAG repeats ranged from 22 to 37. Two other individuals with 38 CAG repeats showed no clinical signs at the time of examination (IV-6, age 37 years in 2007; and IV-7, age 35 years in 2007). The age of onset in the three affected individuals who carried 39 CAG repeats (II-5, IV-16 and IV-17) ranged from 20 to 39 years. Another carrier of 39 CAG repeats (IV-10) showed no clinical signs in 2007, at age 43 years. One of the two individuals who carried 40 CAG repeats had an age at onset of 37 years (IV-12). The other (IV-13) had no clinical signs in 2007, at age 43 years. These observations showed that repeat length alone cannot account for age of onset in this family. Conversely, it is not possible to predict when, or if, the unaffected carriers of expanded CAG repeats will eventually show clinical signs.

Some researches suggested that CAA interruption can lead to phenotypical variation.[23,24] The results of Sobczak *et al.*[25] showed that the CAA interruptions are major determinants of the CAG repeat folding in the SCA2 transcripts. The SCA2 transcripts interrupted by the CAA should generate shorter branched hairpins and the uninterrupted repeats transcripts form single slippery hairpins. The patients who carried SCA2 expansions with and without interruptions show two different phenotypes.[23,24] It may be caused by the different CAG repeat folding that would interact differently with double-stranded RNA binding proteins and interfere with mRNA transcription or translation.[24] That structural organization of CAG expansions with interruption associate with phenotypic variation has been also reported in other neurodegenerative disorders such as SCA1 (see ref. 26). In our family, all patients carried the CAG expansions with one CAA interruption, but showed two different phenotypes. The patients IV-4 and IV-8 showed more ataxia symptoms than the other patients. Especially, patient IV-4 had no response to the levodopa treatment and had marked cerebellar atrophy on MRI. The symptoms of IV-4 made him look more like the typical SCA2. Therefore, the phenotypic variation in our family may be caused by other unknown reason such as co-effect of *SCA2* gene and some modifier gene, rather than the different CAA interruption.

The SCA2 CAG repeat is highly unstable through intergenerational transmission, with a tendency to expand. One study reported that there are 27 families' SCA2 CAG repeats changed in length among 32 SCA2 families, with a mean increase of 2.2 repeat units.[27] In this family, we observed eight transmissions of an expanded SCA2 CAG repeat with no increase in repeat length. Six transmissions yielded no change, whereas two transmissions yielded contractions. As blood samples from several older patients were not collected, we cannot know exactly which SCA2 CAG repeat increased through intergenerational transmission. The explanation for the relative instability in the

family may include genetic or epigenetic factors. A previous study defined the range of the normal SCA2 allele size as 17–31 CAG repeats, whereas full pathogenic mutations had 36–64 repeats.[28] Two unaffected family members who carried the contracted CAG repeat had borderline mutations of 34 CAG repeats (III-13, 45 years of age in 2007; and III-14, 38 years of age in 2007), although 34 CAG repeats were found in some SCA2 patients.[29]

Our linkage analysis revealed two positive regions, one at chromosome 12q24.1 and one at chromosome 5q13.3. On chromosome 12, the mutated *ATXN2* gene, which causes SCA2, is located in the middle of the linkage-positive region. This demonstrates the accuracy of the detection methods and shows that the positive regions are reliable. As the disease gene of SCA2 was located to chromosome 12q23-24.1 (see ref. 30), most of the reports about parkinsonism-predominant SCA2 was based on case cohorts. The linkage study in our family strengthened that the parkinsonism-predominant SCA2 carried the same pathogenic gene as the typical SCA2 from the whole genome perspective. We assume that this parkinsonism-predominant SCA2 family shares a disease locus with other standard SCA2 families, but it is possible that one or more modifier genes interact with *ATXN2* to produce clinical signs more similar to parkinsonism. It is difficult to predict whether the other positive region at 5q13.3 is a real positive region or an artifact. If it is not an artifact, perhaps there would be a modifier gene harbored in the region. To prove it, more detailed gene mutation analyses in the region or other linkage analyses for additional parkinsonism-predominant SCA2 families need to be performed.

The prevalence of SCA2 among patients with familial parkinsonism ranged from 1.5 to 10% (ref. 12). It is seen occasionally in German[28] and Japanese[10] populations. After Gwinn-Hardy *et al.* described a Chinese American family with only or mainly typical parkinsonism in 2000 (see ref. 11), similar families have been reported. Surprisingly, Lu *et al.*[23] reported that four families with SCA2 were identified among 41 families with familial parkinsonism, about 10% of familial parkinsonism carried the expanded SCA2 CAG repeats in Taiwan people. Therefore, it is possible that the mutation rate of potential modifiers might account for the ethnic differences in the predisposition of parkinsonism-predominant SCA2. Better understanding of factors that determine a predominant parkinsonism phenotype in SCA2 may shed light on the pathogenesis of PD.

ACKNOWLEDGEMENTS

This work was supported by the Chinese National Natural Science Foundation (NO. 30400264) and the Yunnan Science and Technology Program (NO. 2008ZC068M). The authors thank the members of the Chinese family for their interest, support and cooperation in this study.

1 Jankovic, J. Parkinson's disease: clinical features and diagnosis. *J. Neurol. Neurosurg. Psychiatry* **79,** 368–376 (2008).
2 de Rijk, M. C., Tzourio, C., Breteler, M. M., Dartigues, J. F., Amaducci, L., Lopez Pousa, S. *et al.* Prevalence of parkinsonism and Parkinson's disease in Europe: the EUROPARKINSON Collaborative Study. European community concerted action on the epidemiology of Parkinson's disease. *J. Neurol. Neurosurg. Psychiatry* **62,** 10–15 (1997).
3 Polymeropoulos, M. H., Lavedan, C., Leroy, E., Ide, S. E., Dehejia, A., Dutra, A. *et al.* Mutation in the alpha-synuclein gene identified in families with Parkinson's disease. *Science* **276,** 2045–2047 (1997).
4 Singleton, A. B., Farrer, M., Johnson, J., Singleton, A., Hague, S., Kachergus, J. *et al.* alpha-Synuclein locus triplication causes Parkinson's disease. *Science* **302,** 841 (2003).
5 Di Fonzo, A., Tassorelli, C., De Mari, M., Chien, H. F., Ferreira, J., Rohe, C. F. *et al.* Comprehensive analysis of the LRRK2 gene in sixty families with Parkinson's disease. *Europ. J. Hum. Genet.* **14,** 322–331 (2006).
6 Berg, D., Schweitzer, K., Leitner, P., Zimprich, A., Lichtner, P., Belcredi, P. *et al.* Type and frequency of mutations in the LRRK2 gene in familial and sporadic Parkinson's disease*. *Brain* **128,** 3000–3011 (2005).
7 Kitada, T., Asakawa, S., Hattori, N., Matsumine, H., Yamamura, Y., Minoshima, S. *et al.* Mutations in the parkin gene cause autosomal recessive juvenile parkinsonism. *Nature* **392,** 605–608 (1998).
8 Valente, E. M., Abou-Sleiman, P. M., Caputo, V., Muqit, M. M., Harvey, K., Gispert, S. *et al.* Hereditary early-onset Parkinson's disease caused by mutations in PINK1. *Science* **304,** 1158–1160 (2004).
9 Bonifati, V., Rizzu, P., van Baren, M. J., Schaap, O., Breedveld, G. J., Krieger, E. *et al.* Mutations in the DJ-1 gene associated with autosomal recessive early-onset parkinsonism. *Science* **299,** 256–259 (2003).
10 Sasaki, H., Wakisaka, A., Sanpei, K., Takano, H., Igarashi, S., Ikeuchi, T. *et al.* Phenotype variation correlates with CAG repeat length in SCA2–a study of 28 Japanese patients. *J. Neurol. Sci.* **159,** 202–208 (1998).
11 Gwinn-Hardy, K., Chen, J. Y., Liu, H. C., Liu, T. Y., Boss, M., Seltzer, W. *et al.* Spinocerebellar ataxia type 2 with parkinsonism in ethnic Chinese. *Neurology* **55,** 800–805 (2000).
12 Furtado, S., Payami, H., Lockhart, P. J., Hanson, M., Nutt, J. G., Singleton, A. A. *et al.* Profile of families with parkinsonism-predominant spinocerebellar ataxia type 2 (SCA2). *Mov. Disord.* **19,** 622–629 (2004).
13 Shan, D. E., Soong, B. W., Sun, C. M., Lee, S. J., Liao, K. K. & Liu, R. S. Spinocerebellar ataxia type 2 presenting as familial levodopa-responsive parkinsonism. *Ann. Neurol.* **50,** 812–815 (2001).
14 Lu, C. S., Wu Chou, Y. H., Yen, T. C., Tsai, C. H., Chen, R. S. & Chang, H. C. Dopa-responsive parkinsonism phenotype of spinocerebellar ataxia type 2. *Mov. Disord.* **17,** 1046–1051 (2002).
15 Furtado, S., Farrer, M., Tsuboi, Y., Klimek, M. L., de la Fuente-Fernandez, R., Hussey, J. *et al.* SCA-2 presenting as parkinsonism in an Alberta family: clinical, genetic, and PET findings. *Neurology* **59,** 1625–1627 (2002).
16 Modoni, A., Contarino, M. F., Bentivoglio, A. R., Tabolacci, E., Santoro, M., Calcagni, M. L. *et al.* Prevalence of spinocerebellar ataxia type 2 mutation among Italian Parkinsonian patients. *Mov. Disord.* **22,** 324–327 (2007).
17 Ruschendorf, F. & Nurnberg, P. ALOHOMORA: a tool for linkage analysis using 10 K SNP array data. *Bioinformatics* **21,** 2123–2125 (2005).
18 Abecasis, G. R., Cherny, S. S., Cookson, W. O. & Cardon, L. R. GRR: graphical representation of relationship errors. *Bioinformatics* **17,** 742–743 (2001).
19 O'Connell, J. R. & Weeks, D. E. PedCheck: a program for identification of genotype incompatibilities in linkage analysis. *Am. J. Hum. Genet.* **63,** 259–266 (1998).
20 Pulst, S. M., Nechiporuk, A., Nechiporuk, T., Gispert, S., Chen, X. N., Lopes-Cendes, I. *et al.* Moderate expansion of a normally biallelic trinucleotide repeat in spinocerebellar ataxia type 2. *Nat. Genet.* **14,** 269–276 (1996).
21 Giunti, P., Sabbadini, G., Sweeney, M. G., Davis, M. B., Veneziano, L., Mantuano, E. *et al.* The role of the SCA2 trinucleotide repeat expansion in 89 autosomal dominant cerebellar ataxia families. Frequency, clinical and genetic correlates. *Brain* **121** (Part 3), 459–467 (1998).
22 Geschwind, D. H., Perlman, S., Figueroa, C. P., Treiman, L. J. & Pulst, S. M. The prevalence and wide clinical spectrum of the spinocerebellar ataxia type 2 trinucleotide repeat in patients with autosomal dominant cerebellar ataxia. *Am. J. Hum. Genet.* **60,** 842–850 (1997).
23 Lu, C. S., Wu Chou, Y. H., Kuo, P. C., Chang, H. C. & Weng, Y. H. The parkinsonian phenotype of spinocerebellar ataxia type 2. *Arch. Neurol.* **61,** 35–38 (2004).
24 Charles, P., Camuzat, A., Benammar, N., Sellal, F., Destee, A., Bonnet, A. M. *et al.* Are interrupted SCA2 CAG repeat expansions responsible for parkinsonism? *Neurology* **69,** 1970–1975 (2007).
25 Sobczak, K. & Krzyzosiak, W. J. CAG repeats containing CAA interruptions form branched hairpin structures in spinocerebellar ataxia type 2 transcripts. *J. Biol. Chem.* **280,** 3898–3910 (2005).
26 Lin, J. X., Ishikawa, K., Sakamoto, M., Tsunemi, T., Ishiguro, T., Amino, T. *et al.* Direct and accurate measurement of CAG repeat configuration in the ataxin-1 (ATXN-1) gene by 'dual-fluorescence labeled PCR-restriction fragment length analysis'. *J. Hum. Genet.* **53,** 287–295 (2008).
27 Cancel, G., Durr, A., Didierjean, O., Imbert, G., Burk, K., Lezin, A. *et al.* Molecular and clinical correlations in spinocerebellar ataxia 2: a study of 32 families. *Hum. Mol. Genet.* **6,** 709–715 (1997).
28 Riess, O., Laccone, F. A., Gispert, S., Schols, L., Zuhlke, C., Vieira-Saecker, A. M. *et al.* SCA2 trinucleotide expansion in German SCA patients. *Neurogenetics.* **1,** 59–64 (1997).
29 Almaguer-Mederos, L. E., Falcon, N. S., Almira, Y. R., Zaldivar, Y. G., Almarales, D. C., Gongora, E. M. *et al.* Estimation of the age at onset in spinocerebellar ataxia type 2 Cuban patients by survival analysis. *Clin. Genet.* **78,** 169–174.
30 Gispert, S., Twells, R., Orozco, G., Brice, A., Weber, J., Heredero, L. *et al.* Chromosomal assignment of the second locus for autosomal dominant cerebellar ataxia (SCA2) to chromosome 12q23-24.1. *Nat. Genet.* **4,** 295–299 (1993).

ELSEVIER

Neurobiology of Aging 32 (2011) 2108.e1–2108.e5

NEUROBIOLOGY OF AGING

www.elsevier.com/locate/neuaging

Genetic Reports Abstracts

Role of sepiapterin reductase gene at the PARK3 locus in Parkinson's disease

Manu Sharma[a,b,*], Demetrius M. Maraganore[c], John P.A. Ioannidis[d,e], Olaf Riess[f], Jan O. Aasly[g], Grazia Annesi[h], Nadine Abahuni[i], Anna Rita Bentivoglio[j], Alexis Brice[k], Christine Van Broeckhoven[l,m], Marie-Christine Chartier-Harlin[n], Alain Destée[n], Ana Djarmati[o], Alexis Elbaz[p], Matthew Farrer[q], Carlo Ferrarese[r], J. Mark Gibson[s,t], Suzana Gispert[i], Nobutaka Hattori[u], Barbara Jasinska-Myga[v], Christine Klein[o], Suzanne Lesage[k], Timothy Lynch[s,t], Peter Lichtner[w], Jean-Charles Lambert[x], Anthony E. Lang[y], George D. Mellick[z,aa], Francesa De Nigris[j], Grzegorz Opala[v], Aldo Quattrone[bb], Chiara Riva[r], Ekaterina Rogaeva[cc], Owen A. Ross[dd], Wataru Satake[ee], Peter A. Silburn[z,aa], Jessie Theuns[l,m], Tatsushi Toda[dd], Hiroyuki Tomiyama[t], Ryan J. Uitti[ff], Karin Wirdefeldt[gg], Zbigniew Wszolek[ff], Thomas Gasser[a,b], Rejko Krüger[a,b], for the Genetic Epidemiology of Parkinson's Disease Consortium

[a] *Center of Neurology and Hertie-Institute for Clinical Brain Research, University of Tübingen, Tuebingen, Germany*
[b] *DZNE-Geman Centre for Neurodegenerative Diseases, Tuebingen, Germany*
[c] *Department of Neurology North Shore University Health System, IL, USA*
[d] *Department of Hygiene and Epidemiology, University of Ioannina School of Medicine, Ioannina, Greece*
[e] *Stanford Prevention Research Centre, Stanford, CA, USA*
[f] *Department of Medical Genetics, University of Tübingen, Germany*
[g] *Department of Neurology, St. Olav's hospital and NTNU, Trondheim, Norway*
[h] *Institute of Neurological Sciences, National Research Council, Cosenza, Italy*
[i] *Department of Neurology, Goethe University, Frankfurt am Main, Germany*
[j] *Department of Neurology, Catholic University, Rome, Italy*
[k] *INSERM, UMR_S975, Université Pierre et Marie Curie-Paris, CNRS, UMR 7225, AP-HP, Pitié-Salpêtrière Hospital, Paris, France*
[l] *Laboratory of Neurogenetics, Institute Born-Bunge, University of Antwerp, Antwerpen, Belgium*
[m] *Neurodegenerative Brain Diseases Group, Department of Molecular Genetics, VIB, Antwerpen, Belgium*
[n] *Inserm UMR837, Centre de Recherche JPArc, Service de Neurologie et de Pathologie du Mouvement CHRU de Lille, University Lille Nord de France*
[o] *Section of Clinical and Molecular Neurogenetics at the Department of Neurology, University of Lübeck, Germany*
[p] *INSERM, Unit 708, F-75013, Paris, France and UPMC Univ Paris 06, U708, Neuroepidemiology, F-75005, Paris, France*
[q] *Department of Genetics, University of British Columbia, Vancouver, BC, Canada*
[r] *Department of Neuroscience-Section of Neurology, University of Milano-Bicocca San Gerardo Hospital, Monza, Italy*
[s] *The Dublin Neurological Institute at the Mater Misericordiae University Hospital, and Conway Institute, University College Dublin, Ireland*
[t] *Department of Neurology, Royal Victoria Hospital, Belfast, Ireland*
[u] *Department of Neurology, Juntendo University School of Medicine, Tokyo, Japan*
[v] *Department of Neurology, Medical University of Silesia, Katowice, Poland*
[w] *Helmholtz Zentrum München, German Research Centre for Environmental Health (Gmbh), Neuherberg, Germany*
[x] *INSERM U744, Institut Pasteur de Lille, Université Lille Nord de France, UDSL, Lille, France*
[y] *Movement Disorders Centre, Toronto Western Hospital, University of Toronto, Toronto, Canada*
[z] *Eskitis Institute for Cell and Molecular Therapies, Griffith University, Nathan, QLD, Australia*
[aa] *University of Queensland, Centre for Clinical Research, Royal Brisbane Hospital*
[bb] *Institute of Neurology, University Magna Graecia, Catanzaro, Italy*
[cc] *Tanz Centre for Research in Neurodegenerative Diseases, Department of Medicine, University of Toronto, Toronto, Canada*
[dd] *Department of Neuroscience, Mayo Clinic, Jacksonville, FL, USA*
[ee] *Division of Neurology/Molecular Brain Science, Kobe University Graduate School of Medicine, Kobe, Japan*
[ff] *Department of Neurology, Mayo Clinic, Jacksonville, FL, USA*
[gg] *Department of Medical Epidemiology and Biostatistics, Karolinska Institutet, Stockholm, Sweden*

Received 23 December 2010; received in revised form 15 April 2011; accepted 30 May 2011

doi:10.1016/j.neurobiolaging.2011.05.024

Abstract

Sepiapterin reductase (*SPR*) gene is an enzyme which catalyses the final step of tetrahydrobiopterin synthesis (BH4) and was implicated in Parkinson's disease (PD) pathogenesis as a candidate gene for PARK3 locus. A number of studies yielded association of the PARK3 locus with PD, and *SPR* knockout mice were shown to display parkinsonian features. To evaluate the role of *SPR* gene polymorphisms in diverse populations in PD, we performed collaborative analyses in the Genetic Epidemiology of Parkinson Disease (GEO-PD) Consortium. A total of 5 single nucleotide polymorphisms (3 in the promoter region and 2 in the 3′ untranslated region [UTR]) were genotyped. Fixed as well as random effect models were used to provide summary risk estimates of *SPR* variants. A total of 19 sites provided data for 6547 cases and 9321 controls. Overall odds ratio estimates varied from 0.92 to 1.01. No overall association with the *SPR* gene using either fixed effect or random effect model was observed in the studied population. I^2 Metric varied from 0% to 36.2%. There was some evidence for an association for participants of North European/Scandinavian descent with the strongest signal for rs1876487 (odds ratio = 0.82; p value = 0.003). Interestingly, families which were used to map the PARK3 locus, have Scandinavian ancestry suggesting a founder effect. In conclusion, this large association study for the *SPR* gene revealed no association for PD worldwide. However, taking the initial mapping of the PARK3 into account, the role of a population-specific effect warrants consideration in future studies.

Keywords: Parkinson disease; *SPR*; PARK3; PD genetic studies; PD-GWAS

1. Introduction

We performed a large multicenter collaborative study among the Genetic Epidemiology of Parkinson's Disease (GEO-PD) Consortium sites to assess the world-wide the role of common variation in the *SPR* gene in Parkinson's disease (PD). This large study includes over 15,868 subjects from 19 sites representing 14 countries from 4 continents (supplementary material).

2. Methods

A total of 19 teams representing 14 countries and 4 continents agreed to participate and contributed clinical and genotypic data for a total of 15,868 individuals (6547 cases and 9321 controls). A total of 5 single nucleotide polymorphisms (SNPs) were selected for genotyping: rs1396107, rs1567230, rs2421095, rs1876487, and rs1561244 listed in order from 5′ to 3′ end of the gene (Karamohamed et al., 2003; Sharma et al., 2006) (supplementary material).

3. Results

Nineteen sites contributed 6547 cases and 9321 controls. Characteristics of all participating sites are shown in Table 1 (supplementary material). The distribution of allele frequencies of each SNP per site is shown in Supplementary Table 2. The meta-analysis did not reveal nominal significant associations either by random or fixed effect models, with the tentative exception of rs1876487. The summary odds ratio (OR) for rs1876487 was 0.95 (95% confidence interval, 0.89–1.00) with a p value of 0.05, uncorrected for multiple testing (Table 1 and supplementary material).

4. Discussion

This very large association study of common variants in the *SPR* gene with PD has revealed no evidence of association world-wide and it excludes large effects for any of the tested variants (supplementary material). Although most genetic association studies typically consider all European populations to share some common ancestry, a recent study established direct correlation between genetic makeup and the geographic location from which samples are ascertained within the European continent. This has also been shown in PD genetics, where in a recently published Genome-Wide Association Study (GWAS) on PD the authors observed a frequency gradient and differential genetic impact for SNP rs3129882 within European population for human leukocyte antigen (HLA) locus (supplementary material). Thus it is conceivable that rs1876487 and/or rs1567230 (D' = 1.0; r^2 = 0.29) may modulate the disease susceptibility only in populations from Northern European descent. Furthermore, haploytpe analysis restricted to North European population showed suggestive evidence of association for haplotype (rs2421095-rs1876487-rs1561244; odds ratio, 0.57; p-value 0.07), again suggesting the role of founder effect for PARK3 locus in North European/Scandinavian populations. Acknowledging these caveats, our study is large enough to suggest that these variants are unlikely to be a clinically important determinant of PD risk world-wide and future efforts should focus specifically on Northern European populations.

Disclosure statement

All authors have reported no actual or potential conflict of interest.

* Corresponding author at: Hertie-Insitute of Clinical Brain Research, Department of Neurology, University of Tuebingen, Hoppe-Seyler-Str. 3, 72076 Tübingen, Germany. Tel.: +49 7071 29 81 968; fax: +49 7071 29 4620.

E-mail address: manu.sharma@uni-tuebingen.de (M. Sharma).

Table 1
Summary effect estimates and confidence interval for *SPR* gene

SNP	Site	Overall			North European/Scandinavian		
		RE OR (95% CI)	FE OR (95% CI)	Het p (I^2)	RE OR (95% CI)	FE OR (95% CI)	Het p (I^2)
rs1396107	17	0.97 (0.90–1.03)	0.97 (0.90–1.03)	0.80 (0%)	0.87 (0.76–0.99)	0.87 (0.76–0.99)	0.42 (0%)
rs1567230	18	0.93 (0.82–1.04)	0.92 (0.83–1.03)	0.29 (14%)	0.75 (0.59–0.94)	0.74 (0.60–0.91)*	0.31 (13%)
rs2421095	19	0.93 (0.84–1.04)	0.93 (0.85–1.01)	0.18 (21%)	0.78 (0.63–0.96)	0.78 (0.63–0.96)	0.68 (0%)
rs1876487	18	0.94 (0.89–1.00)	0.94 (0.89–1.00)	0.46 (0%)	0.83 (0.72–0.96)	0.82 (0.72–0.93)*	0.33 (12%)
rs1561244	17	1.01 (0.91–1.12)	1.00 (0.92–1.08)	0.07 (36%)	0.88 (0.72–1.08)	0.85 (0.73–1.00)	0.23 (30%)

Key: CI, confidence interval; FE, fixed effects; Het, heterogeneity (Q statistic); OR, odds ratio; RE, random effects.
* $p < 0.01$.

Appropriate approval and procedures were used concerning human subjects.

Acknowledgements

Australia: From the Queensland Parkinson's Project: R.S. Boyle and A. Sellbach (Princess Alexandra Hospital, Brisbane), J.D. O'Sullivan (Royal Brisbane and Women's Hospital, Brisbane), G.T. Sutherland, G.A. Siebert and N.N.W. Dissanayaka (Eskitis Institute for Cell and Molecular Therapies, Griffith University, Nathan, QLD).

Belgium: Christine Van Broeckhoven, Ph.D., D.Sc. (Neurodegenerative Brain Diseases Group, Department of Molecular Genetics, VIB; and Laboratory of Neurogenetics, Institute Born-Bunge, University of Antwerp; Antwerpen), Jessie Theuns, PhD (Neurodegenerative Brain Diseases Group, Department of Molecular Genetics, VIB; and Laboratory of Neurogenetics, Institute Born-Bunge, University of Antwerp; Antwerpen), David Crosiers, M.D. (Neurodegenerative Brain Diseases Group, Department of Molecular Genetics, VIB; and Laboratory of Neurobiology, Institute Born-Bunge, University of Antwerp; and Department of Neurology, University Hospital Antwerp; Antwerpen), Barbara Pickut, M.D. (Department of Neurology, University Hospital Antwerp; Antwerpen), Sebastiaan Engelborghs, M.D., Ph.D. (Laboratory of Neurochemistry and Behavior, Institute Born-Bunge, University of Antwerp; and Department of Neurology and Memory Clinic, Hospital Network Antwerp Middelheim and Hoge Beuken; Antwerpen), Bram Meeus (Neurodegenerative Brain Diseases Group, Department of Molecular Genetics, VIB; and Laboratory of Neurogenetics, Institute Born-Bunge, University of Antwerp; Antwerpen), Peter P. De Deyn, M.D., Ph.D. (Laboratory of Neurochemistry and Behavior, Institute Born-Bunge, University of Antwerp; and Department of Neurology and Memory Clinic, Hospital Network Antwerp Middelheim and Hoge Beuken; Antwerpen), Patrick Cras, M.D., Ph.D. (Laboratory of Neurobiology, Institute Born-Bunge, University of Antwerp; and Department of Neurology, University Hospital Antwerp; Antwerpen). Funding: The research at this site was in part supported by the Special Research Fund of the University of Antwerp, the Medical Research Foundation Antwerp and Neurosearch, the Research Foundation Flanders (FWO), the Flanders government agency for Innovation by Science and Technology (IWT), the Foundation for Alzheimer Research (SAO/FRMA), the Belgian Science Policy Office Interuniversity Attraction Poles (IAP) Program P6/43, a Methusalem Excellence Grant of the Flanders Government and, and the Alzheimer's Association USA,. B.M. received a Ph.D. fellowship of the IWT and D.C. of the FWO; J.T. received a FWO postdoctoral fellowship.

Canada: Ekaterina Rogaeva, Ph.D. (Tanz Centre for Research in Neurodegenerative Diseases, Department of Medicine, Division of Neurology, University of Toronto; ON, Canada); Anthony E. Lang, M.D., Movement Disorders Centre, Toronto Western Hospital, University of Toronto, Toronto, ON, Canada.

France: From the French Parkinson's Disease Genetics Study Group: Y. Agid, M. Anheim, A.-M. Bonnet, M. Borg, A. Brice, E. Broussolle, J.C. Corvol, P. Damier, A. Destée, A. Dürr, F. Durif, S. Lesage, E. Lohmann, P. Pollak, O. Rascol, F. Tison, C. Tranchant, F. Viallet, and M. Vidailhet. Also, Christophe Tzourio (Inserm U708, Paris), Philippe Amouyel (Inserm U744, Lille), Marie-Anne Loriot (Inserm UMRS775, Paris). Eugénie Mutez (Inserm UMR837, Service de Neurologie et de Pathologie du Mouvement CHRU de Lille, University Lille Nord de France), Aurélie Duflot, (UMR837 Inserm-University Lille 2, CHRU de Lille), Jean-Philippe Legendre (Service de Neurologie et Pathologie du Mouvement, Clinique de Neurologie du CHU de Lille), Nawal Waucquier (Service de Neurologie et Pathologie du Mouvement, Clinique de Neurologie du CHU de Lille), the 2 Centres de Ressources Biologiques (IPL-Lille, CHRU-Lille) and its scientific committee (AD, MCCH, P. Amouyel, F. Pasquier, R. Bordet). Funding: This work is supported by the French National Agency of Research (ANR-08-MNP-012). Lille: Financial support from CHRU de Lille, University Lille 2, Inserm, French Ministry PHRCs (1994/, 2002/1918, 2005/1914), Association France Parkinson (2005), Fondation de France 2004-013306, Fondation de la Recherche Médicale (2006), P.P.F. (Synucléothèque 2005-2009),

Germany: Thomas Gasser, M.D., (Department of Neurology, University Hospital Tuebingen), Olaf Riess, M.D. (Department of Neurology, University Hospital Tuebingen),

Daniela Berg, M.D., (Department of Neurology, University Hospital Tuebingen), Claudia Schulte, M.Sc. (Department of Neurology, University Hospital Tuebingen), Christine Klein, M.D. (Section of Clinical and Molecular Neurogenetics at the Department of Neurology, University of Lübeck), Ana Djarmati, Ph.D. (Department of Neurology, University of Lübeck), Johann Hagenah, M.D. (Department of Neurology, University of Lübeck), Katja Lohmann, Ph.D. (Section of Clinical and Molecular Neurogenetics at the Department of Neurology, University of Lübeck), Georg Auburger, M.D. (Department of Neurology, Goethe University Frankfurt am Main, Germany), Rüdiger Hilker, M.D. (Department of Neurology, Goethe University Frankfurt am Main, Germany), Simone van de Loo, M.D. (Department of Neurology, Goethe University Frankfurt am Main, Germany).

Greece: Efthimios Dardiotis, M.D. (Department of Neurology, Faculty of Medicine, University of Thessaly and Institute of Biomedical Research & Technology, CERETETH, Larissa), Vaia Tsimourtou (Department of Neurology, Faculty of Medicine, University of Thessaly, Larissa), Styliani Ralli (Department of Neurology, Faculty of Medicine, University of Thessaly, Larissa), Persa Kountra, M.D. (Department of Neurology, Faculty of Medicine, University of Thessaly, Larissa), Konstantinos Aggelakis (Institute of Biomedical Research & Technology, CERETETH, Larissa).

Japan: Nobutaka Hattori, M.D., Ph.D. (Department of Neurology, Juntendo University School of Medicine, Tokyo), Hiroyuki Tomiyama, M.D., Ph.D. (Department of Neurology, Juntendo University School of Medicine, Tokyo), Manabu Funayama, Ph.D. (Department of Neurology, and Research Institute for Diseases of Old Age, Graduate School of Medicine, Juntendo University, Tokyo), Hiroyo Yoshino, B.S. (Research Institute for Diseases of Old Age, Graduate School of Medicine, Juntendo University, Tokyo), Yuanzhe Li, M.D., Ph.D. (Department of Neurology, Juntendo University School of Medicine, Tokyo), Yoko Imamichi (Department of Neurology, Juntendo University School of Medicine, Tokyo), Tatsushi Toda, M.D. (Division of Neurology/Molecular Brain Science, Kobe University Graduate School of Medicine, Kobe, Japan), Wataru Satake (Division of Neurology/Molecular Brain Science, Kobe University Graduate School of Medicine, Kobe, Japan). Funding: This work was supported by a grant from the Japanese Ministry of Education, Culture, Sports, Science and Technology, Grants-in-Aid for Scientific Research (to HT: 21591098; to NH: 090052131), for Scientific Research on Priority Areas (to NH: 08071510), and for Young Scientists (to MF: 22790829).

Ireland: Prof. Tim Lynch, FRCPI, FRCP (The Dublin Neurological Institute at the Mater Misericordiae University Hospital, Clinical Investigator at the Conway Institute, University College Dublin, Ireland), and Dr J. Mark Gibson, M.D. (Department of Neurology, Royal Victoria Hospital, Belfast, Ireland).

Italy: Enza Maria Valente, M.D., Ph.D. (IRCCS, Casa Sollievo della Sofferenza Hospital, Mendel Institute, San Giovanni Rotondo), Alessandro Ferraris, M.D., (IRCCS, Casa Sollievo della Sofferenza Hospital, Mendel Institute, San Giovanni Rotondo), Bruno Dallapiccola (Mendel Institute, Casa Sollievo della Sofferenza Hospital, Rome), Tamara Ialongo, M.D., Ph.D. (Institute of Neurology, Catholic University, Rome), Laura Brighina, M.D., Ph.D. (Department of Neurology, Ospedale San Gerarado, Monza, Italy), Barbara Corradi, Ph.D. (Department of Paediatrics, University of Milano-Bicocca, Monza), Roberto Piolti, M.D. (Department of Neurology, Ospedale San Gerardo, Monza, Italy), Patrizia Tarantino, Ph.D. (Institute of Neurological Sciences, National Research Council), and Ferdinanda Annesi, Ph.D. (Institute of Neurological Sciences, National Research Council).

Norway: J. Aasly, M.D. (Department of Neurology, University of Trondheim, Norway).

Poland: Grzegorz Opala, M.D., Ph.D. (Department of Neurology, Aging, Degenerative and Cerebrovascular Disorders, Medical University of Silesia, Katowice), Barbara Jasinska-Myga, M.D., Ph.D. (Department of Neurology, Aging, Degenerative and Cerebrovascular Disorders, Medical University of Silesia, Katowice), Gabriela Klodowska-Duda, M.D., Ph.D. (Department of Neurology, Aging, Degenerative and Cerebrovascular Disorders, Medical University of Silesia, Katowice), Magdalena Boczarska-Jedynak, M.D., Ph.D. (Department of Neurology, Aging, Degenerative and Cerebrovascular Disorders, Medical University of Silesia, Katowice).

Singapore: Eng King Tan, M.D., Ph.D. (National Medical and Biomedical Research Councils, and the Duke-NUS Graduate Medical School, Singapore Millenium Foundation).

Sweden: Andrea Carmine Belin, Ph.D. (Department of Neuroscience, Karolinska Institutet, Stockholm), Lars Olson, Professor (Department of Neuroscience, Karolinska Institutet, Stockholm), Dagmar Galter, Ph.D. (Department of Neuroscience, Karolinska Institutet, Stockholm), Marie Westerlund, Ph.D. (Department of Neuroscience, Karolinska Institutet, Stockholm), Olof Sydow, Ph.D., (Department of Clinical Neuroscience, Karolinska University Hospital, Stockholm). Also Christer Nilsson, M.D., Ph.D. (Department of Geriatric Psychiatry, Lund University), Andreas Puschmann, M.D. (Department of Neurology, Lund University Hospital, Department of Geriatric Psychiatry, Lund University).

Taiwan: J.J. Lin, M.D., Department of Neurology, Cushang Show-Chwan Hospital, Taiwan.

USA: Demetrius M. Maraganore, M.D. (Department of Neurology, Mayo Clinic, Rochester, MN, USA), J. Eric Ahlskog, Ph.D., M.D. (Department of Neurology, Mayo Clinic, Rochester, MN, USA), Mariza de Andrade, Ph.D.

(Department of Health Sciences Research, Mayo Clinic, Rochester, MN, USA), Timothy G. Lesnick, M.S. (Department of Health Sciences Research, Mayo Clinic, Rochester, MN, USA), and Walter A. Rocca, M.D., M.P.H. (Departments of Neurology and Health Sciences Research, Mayo Clinic, Rochester, MN, USA). Also, Harvey Checkoway, Ph.D. (Department of Environmental and Occupational Health Sciences, University of Washington, Seattle, WA, USA), Owen A. Ross, Ph.D. (Division of Neuroscience, Mayo Clinic, Jacksonville, FL, USA), Zbigniew K. Wszolek, M.D., and Ryan J. Uitti, M.D. (Department of Neurology, Mayo Clinic, Jacksonville, FL, USA). Funding: Z.K.W. is partially supported by the NIH/NINDS 1RC2NS070276, NS057567, P50NS072187, Mayo Clinic Florida (MCF) Research Committee CR programs (MCF #90052018 and MCF #90052030), and the gift from Carl Edward Bolch, Jr., and Susan Bass Bolch (MCF #90052031/PAU #90052).

Funding to investigators was provided by the German Federal Ministry for Education and Research (BMBF, NGFNplus; 01GS08134) to T.G., O.R., and R.K., and Rapid Response Innovation Award from the Michael J. Fox Foundation to M.S.; Grants-in-Aid for Scientific Research (to HT: 21591098), and Grants-in-Aid from the Research Committee of CNS Degenerative Diseases and Perry syndrome (to HT: 22140901) from the Japanese Ministry of Education, Culture, Sports, Science and Technology.

Appendix: A. Supplementary data

Supplementary data associated with this article can be found, in the online version, at doi:10.1016/j.neurobiolaging.2011.05.024.

References

Karamohamed, S., DeStefano, A.L., Wilk, J.B., Shoemaker, C.M., Golbe, L.I., Mark, M.H., Lazzarini, A.M., Suchowersky, O., Labelle, N., Guttman, M., Currie, L.J., Wooten, G.F., Stacy, M., Saint-Hilaire, M., Feldman, R.G., Sullivan, K.M., Xu, G., Watts, R., Growdon, J., Lew, M., Waters, C., Vieregge, P., Pramstaller, P.P., Klein, C., Racette, B.A., Perlmutter, J.S., Parsian, A., Singer, C., Montgomery, E., Baker, K., Gusella, J.F., Fink, S.J., Myers, R.H., Herbert, A., GenePD study, 2003. A haplotype at the PARK3 locus influences onset age for Parkinson's disease: the GenePD study. Neurology 61, 1557–1561.

Sharma, M., Mueller, J.C., Zimprich, A., Lichtner, P., Hofer, A., Leitner, P., Maass, S., Berg, D., Dürr, A., Bonifati, V., De Michele, G., Oostra, B., Brice, A., Wood, N.W., Muller-Myhsok, B., Gasser, T., European Consortium on Genetic Susceptibility in Parkinson's Disease (GSPD), 2006. The sepiapterin reductase gene region reveals association in the PARK3 locus: analysis of familial and sporadic Parkinson's disease in European populations. J. Med. Genet. 43, 557–562.

SAGE-Hindawi Access to Research
Journal of Amino Acids
Volume 2011, Article ID 265084, 10 pages
doi:10.4061/2011/265084

Review Article

The Aggregation Inhibitor Peptide QBP1 as a Therapeutic Molecule for the Polyglutamine Neurodegenerative Diseases

H. Akiko Popiel,[1] James R. Burke,[2] Warren J. Strittmatter,[2] Shinya Oishi,[3] Nobutaka Fujii,[3] Toshihide Takeuchi,[1] Tatsushi Toda,[4] Keiji Wada,[1] and Yoshitaka Nagai[1,5]

[1] *Department of Degenerative Neurological Diseases, National Institute of Neuroscience, National Center of Neurology and Psychiatry, 4-1-1 Ogawa-Higashi, Kodaira, Tokyo 187-8502, Japan*
[2] *Department of Medicine (Neurology) and Deane Laboratory, Duke University Medical Center, Durham, NC 27710, USA*
[3] *Department of Bioorganic Medicinal Chemistry, Kyoto University Graduate School of Pharmaceutical Sciences, Kyoto 606-8501, Japan*
[4] *Division of Neurology/Molecular Brain Science, Kobe University Graduate School of Medicine, Kobe 650-0017, Japan*
[5] *Core Research for Evolutional Science and Technology (CREST), Japan Science and Technology Agency, Saitama 332-0012, Japan*

Correspondence should be addressed to Yoshitaka Nagai, nagai@ncnp.go.jp

Received 31 January 2011; Accepted 4 May 2011

Academic Editor: Andreas Wyttenbach

Misfolding and abnormal aggregation of proteins in the brain are implicated in the pathogenesis of various neurodegenerative diseases including Alzheimer's, Parkinson's, and the polyglutamine (polyQ) diseases. In the polyQ diseases, an abnormally expanded polyQ stretch triggers misfolding and aggregation of the disease-causing proteins, eventually resulting in neurodegeneration. In this paper, we introduce our therapeutic strategy against the polyQ diseases using polyQ binding peptide 1 (QBP1), a peptide that we identified by phage display screening. We showed that QBP1 specifically binds to the expanded polyQ stretch and inhibits its misfolding and aggregation, resulting in suppression of neurodegeneration in cell culture and animal models of the polyQ diseases. We further demonstrated the potential of protein transduction domains (PTDs) for *in vivo* delivery of QBP1. We hope that in the near future, chemical analogues of aggregation inhibitor peptides including QBP1 will be developed against protein misfolding-associated neurodegenerative diseases.

1. Introduction

Neurodegenerative diseases are a group of disorders, which are caused by progressive degeneration of neurons in various areas of the brain specific for each disorder, resulting in various neurological and psychiatric symptoms corresponding to each affected brain area. Few effective therapies have been established to date for these diseases, largely due to the fact that the underlying cause of the neurodegeneration long remained unknown. However, accumulating evidence now indicates that many of these neurodegenerative diseases, including Alzheimer's disease (AD), Parkinson's disease (PD), the polyglutamine (polyQ) diseases, amyotrophic lateral sclerosis, and the prion diseases, share a common pathomechanism (Figure 1). Pathological and biochemical studies have revealed that various protein inclusions accumulate inside and outside of neurons in the diseased brains, such as senile plaques composed of amyloid-β and neurofibrillary tangles composed of tau in AD, and Lewy bodies composed of α-synuclein in PD. Although the significance of these protein inclusions on disease pathology long remained controversial, recent molecular genetics studies revealed that the mutations responsible for the inherited forms of these diseases render the proteins to be prone to misfold and aggregate, or lead to the overproduction of aggregation-prone proteins. Furthermore, not only such genetic mutations, but also multiple environmental factors are thought to trigger the misfolding of otherwise normal proteins, and indeed the sporadic cases of these diseases also exhibit similar protein inclusions in the brain. It is noteworthy that the aggregates composed of different proteins accumulated in the different diseases all have a similar structure, namely, that they are β-sheet-rich amyloid. In addition, genetic animal models

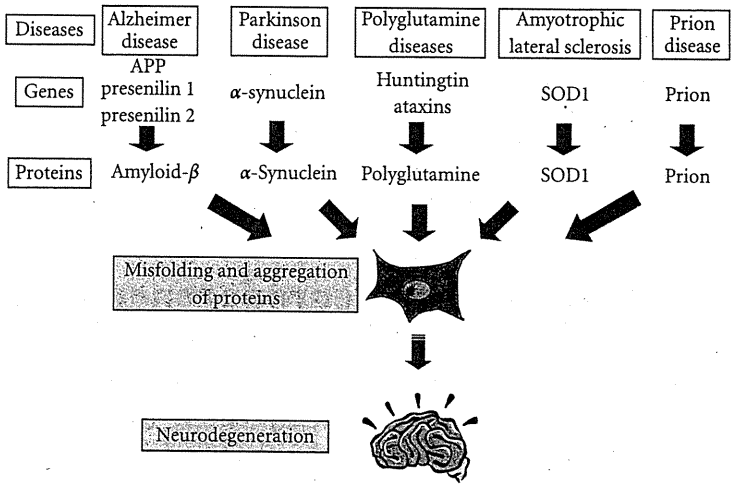

FIGURE 1: Misfolding and abnormal aggregation of proteins as a common molecular pathogenesis of the protein misfolding diseases. The genetic mutations responsible for the inherited forms of various neurodegenerative diseases render the proteins prone to misfold and aggregate, or lead to the overproduction of aggregation-prone proteins, which accumulate as inclusions inside and outside neurons in the diseased brains, and eventually cause neurodegeneration. These facts indicate that the misfolding and abnormal aggregation of proteins are crucial in the pathogenesis of these diseases, which are known as the "protein misfolding diseases."

expressing these aggregation-prone mutant proteins have been found to develop similar protein inclusions as well as neurodegeneration. These facts, taken together, have strongly suggested that the misfolding and abnormal aggregation of proteins are crucial in the pathogenesis of these neurodegenerative diseases, which are hence collectively called the "protein misfolding diseases" [1–3] (Figure 1).

Our group has been working towards establishing therapies for these protein misfolding diseases, with a particular focus on the polyQ diseases because of the following reasons. Firstly, they are determined almost solely by a monogenic mutation and are minorly influenced by environmental factors unlike the other diseases. Furthermore, there is a tight correlation between the severity of the genetic mutation and the disease phenotypes. These special characteristics highlight the polyQ diseases as the most suitable model for the protein misfolding diseases.

In this review, we will introduce our research towards establishing a therapy for the polyQ diseases by targeting the protein misfolding and aggregation, using polyglutamine binding peptide 1 (QBP1), a small biologically active peptide that we identified from combinatorial screening.

2. The Polyglutamine Diseases

Molecular genetics studies on inherited neurodegenerative diseases in the last few decades have revealed a common genetic mutation shared by a group of diseases, namely, an expansion (>40) of the CAG repeat encoding a polyQ stretch in each unrelated disease-causing gene, and hence these diseases are called the polyQ diseases [4, 5]. Currently nine diseases have been found to belong to this group, including Huntington's disease, spinocerebellar ataxia (SCA) type 1, 2, 3, 6, 7, and 17, dentatorubral pallidoluysian atrophy, and spinobulbar muscular atrophy (SBMA) [6–17].

The polyQ diseases share many common characteristics, although the responsible proteins share no particular functional or sequence similarities except for the polyQ stretch. Most of the diseases are inherited through an autosomal dominant manner except for SBMA. The threshold of the polyQ repeat size for disease manifestation is approximately 35–40, except for SCA6, and the length of the polyQ repeat is tightly correlated with the age of onset and severity of the disease. These facts taken together strongly indicate that the expanded polyQ stretch itself causes these diseases via a gain of toxic function mechanism, which is unrelated with the normal function of the host protein. Indeed, expression of an expanded polyQ stretch alone or even an expanded polyQ stretch introduced into an unrelated protein has been shown to cause neurodegeneration in various experimental animal models [18–21].

As a common molecular pathogenesis of the polyQ diseases, it has been proposed that proteins with an expanded polyQ stretch become misfolded and form oligomers and amyloid fibrillar aggregates, and subsequently accumulate as inclusion bodies within neurons, eventually resulting in neurodegeneration (Figure 2) [22–26]. Various cellular proteins have been shown to associate with the polyQ aggregates/inclusion bodies, including transcription factors [27, 28], molecular chaperones [29, 30], cytoskeletal proteins [31], and proteasomal subunits [29], and such abnormal associations are thought to play a role in the disease pathogenesis, through dysfunction of the cellular processes involving these proteins. Accordingly, there have been therapeutic approaches targeting each specific cellular process that is compromised in the disease pathogenesis [23, 32]. However, these attempts result in only limited therapeutic effects, since numerous cellular processes are affected by expression of the expanded polyQ protein [33–36]. In contrast to these downstream events, misfolding and aggregation of the